Molecules at the Reionization Epoch

CO/H2 and OH/CO: from Low Metallicities to High Ionization Rates

Shmuel Bialy & Amiel Sternberg
Tel Aviv University

1409.6724

Basic Question

- During the reionization epoch stars (pop-II) formed in very low metallicity gas clouds
- Pop-II stars in the halo - down to $Z=10^{-4.5}$ (Caffau+12)
- Metal-poor DLAs up to redshift 5 - down to $Z=10^{-2.7}$ (Rafelski+13)

Basic Question

- During the reionization epoch stars (pop-II) formed in very low metallicity gas clouds
- Pop-II stars in the halo - down to $Z=10^{-4.5}$ (Caffau+12)
- Metal-poor DLAs up to redshift 5 - down to $Z=10^{-2.7}$ (Rafelski+13)

What are the chemical properties of dense clouds "GMC-analogues" at low metallicity?

Basic Question

What are the chemical properties of dense clouds “GMC-analogues” at low metallicity?

Basic Question

What are the chemical properties of dense clouds "GMC-analogues" at low metallicity?

Basic Question

What are the chemical properties of dense clouds "GMC-analogues" at low metallicity?

abundances → cooling → star mass

- pop-III to pop-II transition (e.g., Bromm+03, Omukai+05)

Basic Question

What are the chemical properties of dense clouds "GMC-analogues" at low metallicity?

abundances → cooling → star mass

- pop-III to pop-II transition (e.g., Bromm+03, Omukai+05)

atomic & mol. transitions = probes of star-forming gas

- C II 158 μm, CO rotational ladder (mm wave FIR)
- conversion factor α_{CO} → molecular mass

Basic Question

What are the chemical properties of dense clouds “GMC-analogues” at low metallicity?

1. **May be atomic (H) rather than molecular (H_2)**
2. **OH-dominated versus CO-dominated gas**
3. **CO/H_2 variations with Z, ionization rate and density**

Model

- Lyman-Werner band blocked (11.2-13.6 eV)
- CR, X-rays
- FUV (E<11.2 eV)

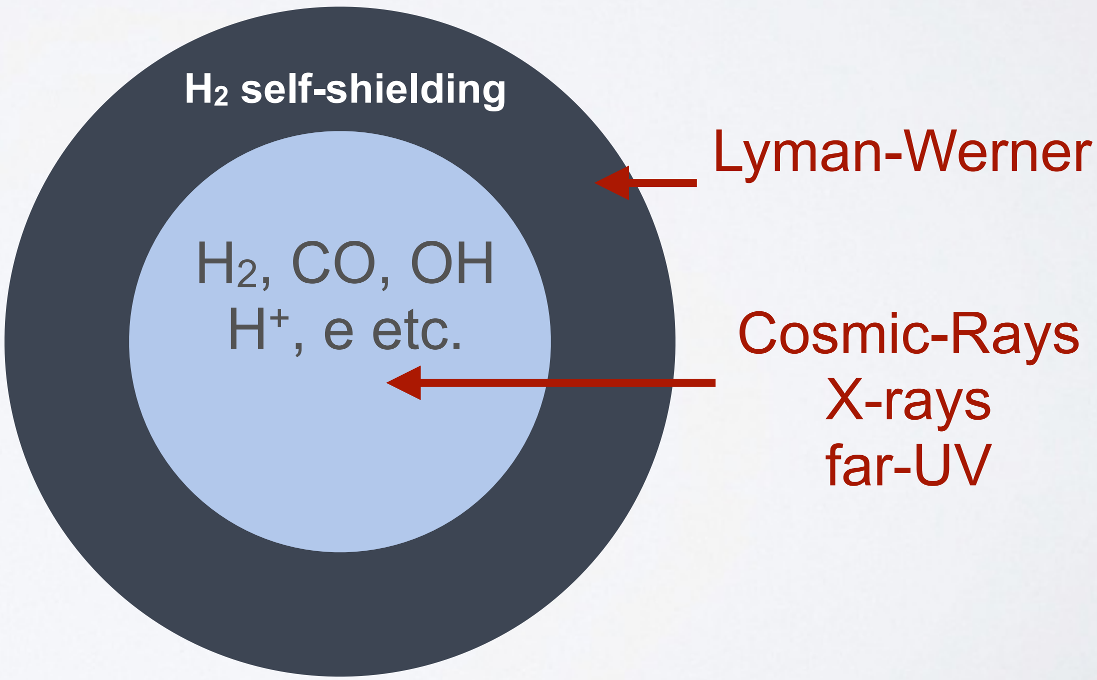

Chemical Model primarily gas phase

Ion-mol. network (+ H_2 on dust α Z)

⇓

Steady state formation destruction eq.

⇓

Species abundances

Hydrogen network

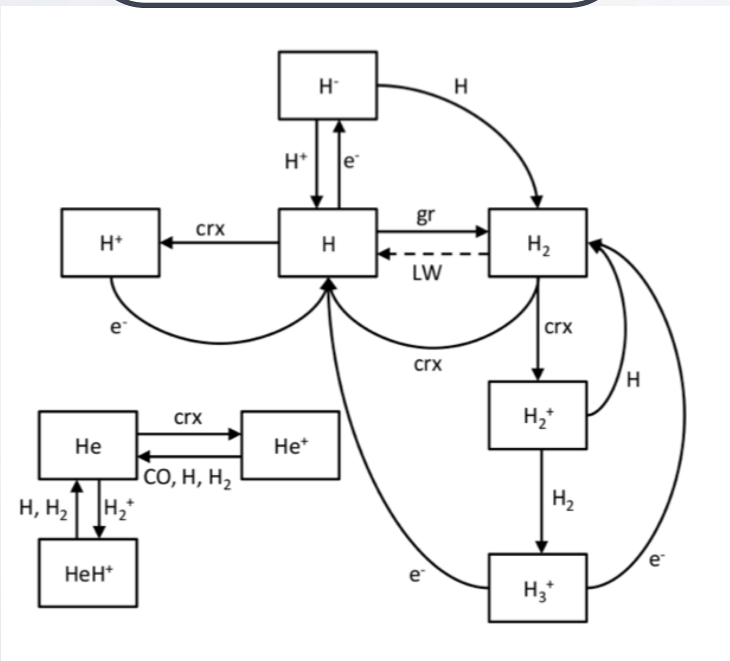

Oxygen network

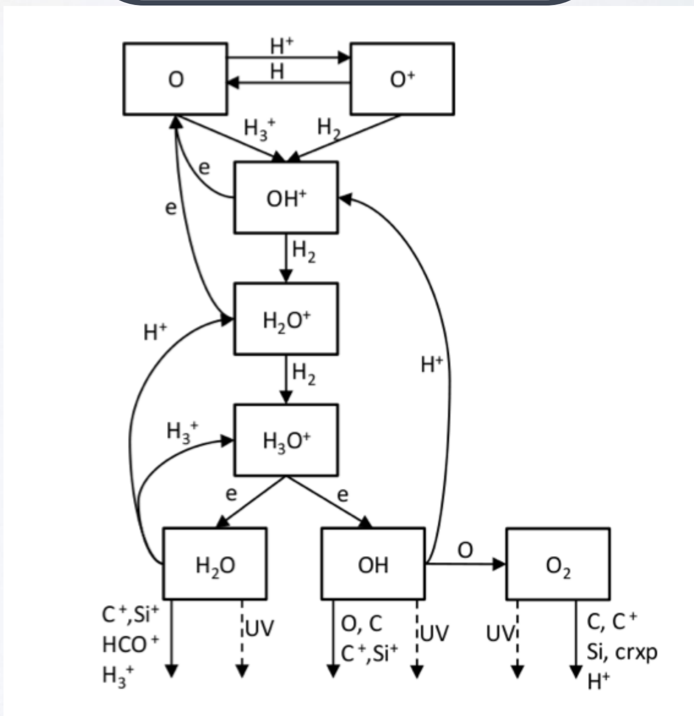

Parameters

- **Z** gas metallicity relative to solar
- **ζ** (s^{-1}) ionization rate (via CR/Xray)
- **n** (cm^{-3}) total hydrogen number density
- **T** (K) temperature
- F_{FUV} (cm^{-3}) far-UV flux

Parameters

Intro

Model

Results

Summary

• **Z**		gas metallicity relative to solar
• **ζ**	(s^{-1})	ionization rate (via CR/Xray)
• **n**	(cm^{-3})	total hydrogen number density
• **T**	(K)	temperature
• F_{FUV}	(cm^{-3})	far-UV flux

- We examine w/o FUV, here I will show FUV=Off
- CO to OH transition - insensitive to FUV
- Weak dependence on T (for 10<T<300 K) - we assume 100 K

Parameters

• **Z**		gas metallicity relative to solar
• **ζ**	(s^{-1})	ionization rate (via CR/Xray)
• **n**	(cm^{-3})	total hydrogen number density
• **T**	(K)	temperature
• F_{FUV}	(cm^{-3})	far-UV flux

- We examine w/o FUV, here I will show FUV=Off
- CO to OH transition - insensitive to FUV
- Weak dependence on T (for 10<T<300 K) - we assume 100 K

The relative abundances $n_i/n_j = f\,(Z\,,\,\zeta/n\,)$

Parameters

2 D parameter space

Z

ζ/n

The relative abundances $n_i/n_j = f\,(Z\,,\,\zeta/n\,)$

Parameters

2 D parameter space

Z

ζ/n

The relative abundances $n_i/n_j = f(Z, \zeta/n)$

1D cuts at fixed ζ/n

$\zeta_{-16}/n_3=1$

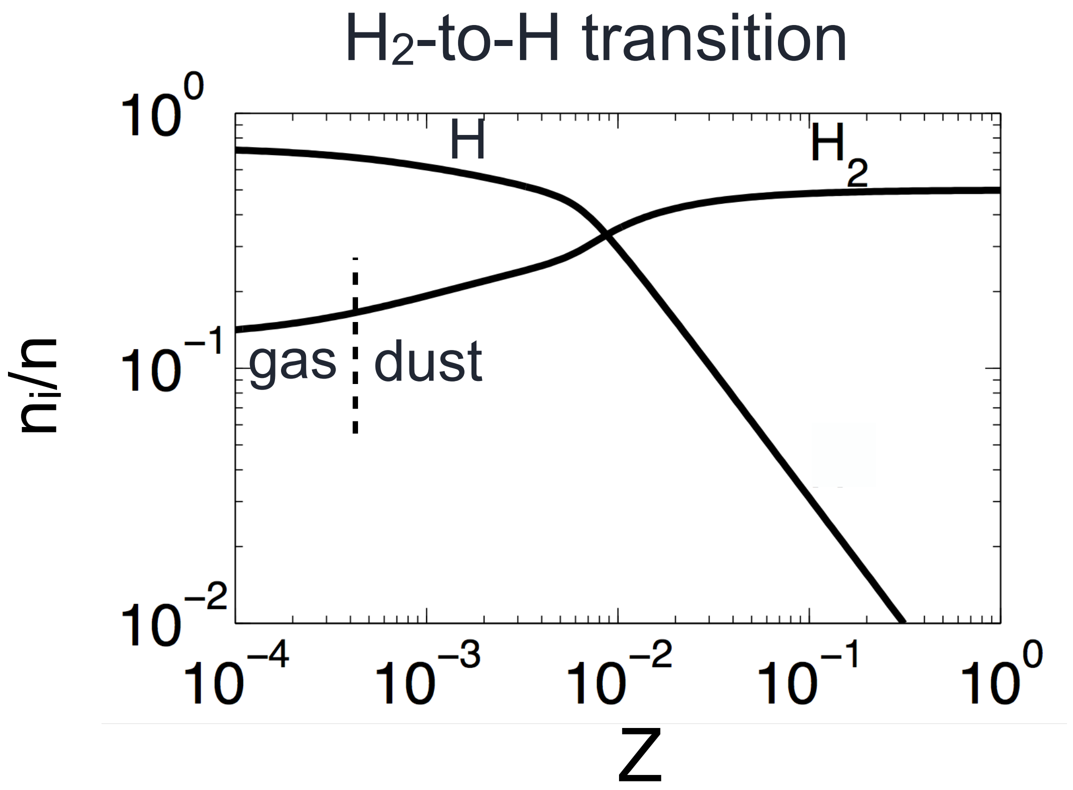

H_2 formation

1. dust grains α Z
2. gas phase

$H + e \rightarrow H^- + \nu$

$H^- + H \rightarrow H_2 + e$

H_2-to-H transition

$Z=10^{-2}$

H_2-to-H transition

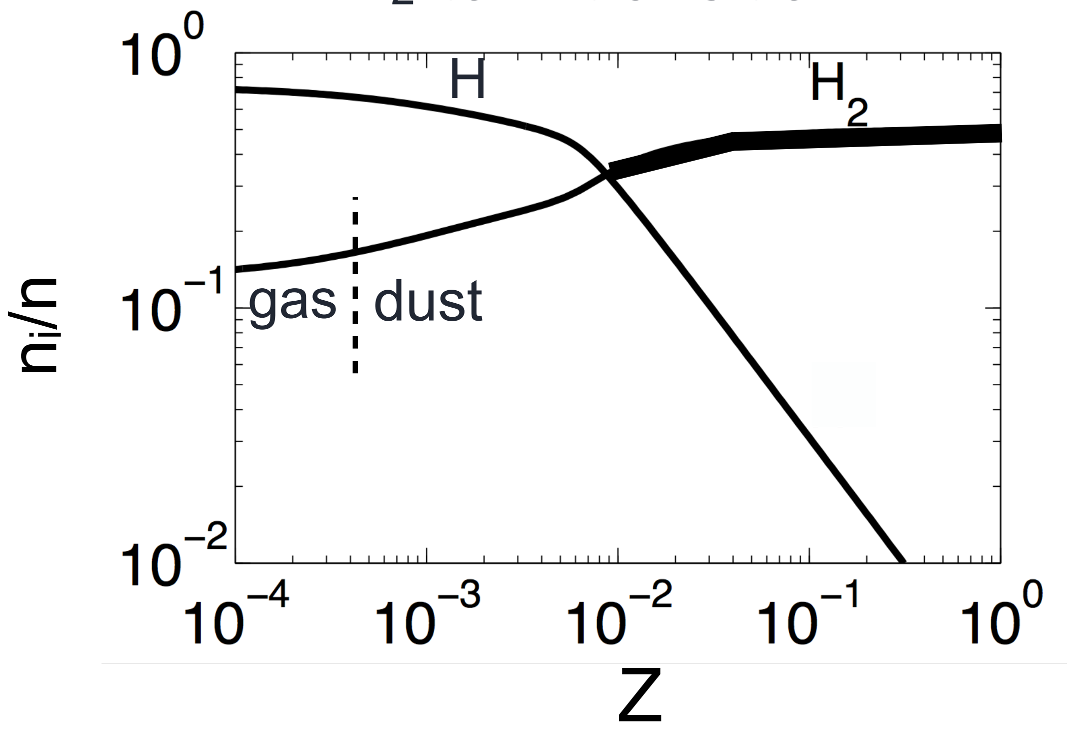

H_2 formation

1. dust grains α Z
2. gas phase

$H + e \rightarrow H^- + \nu$

$H^- + H \rightarrow H_2 + e$

H_2-to-H transition

$Z=10^{-2}$

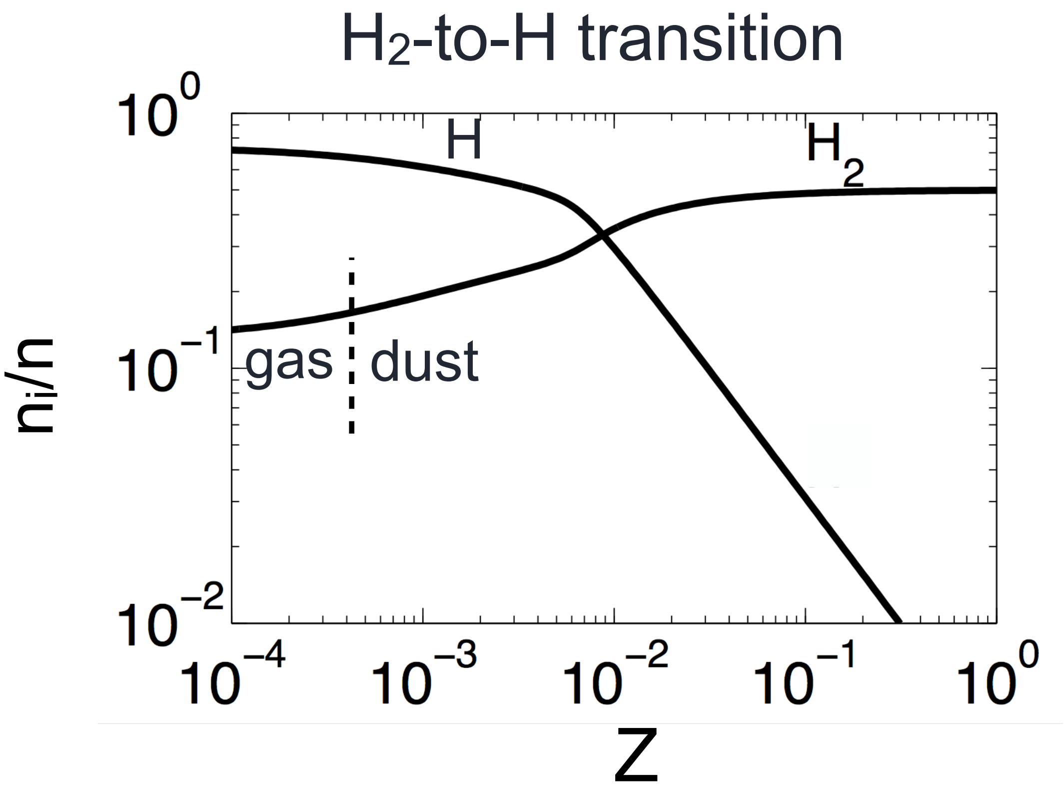

H_2 formation

1. dust grains α Z
2. gas phase

$H + e \rightarrow H^- + v$

$H^- + H \rightarrow H_2 + e$

H$_2$-to-H transition

$Z = 10^{-2}$

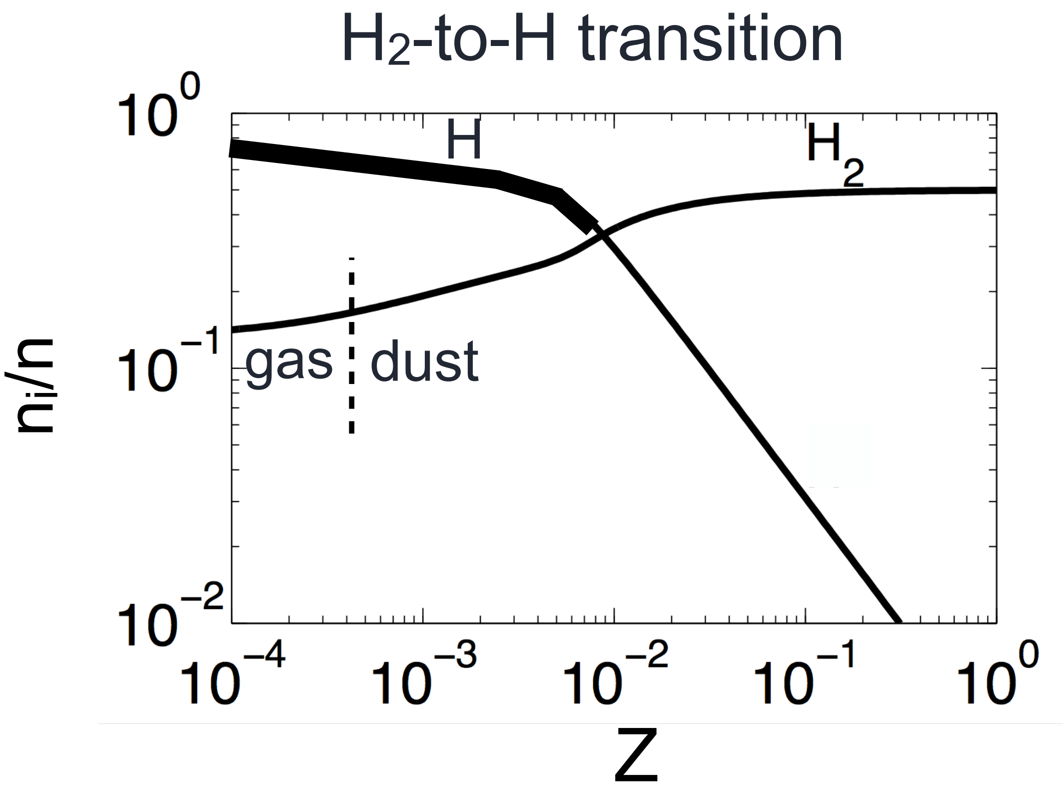

H_2 formation

1. dust grains α Z
2. gas phase

$H + e \rightarrow H^- + v$

$H^- + H \rightarrow H_2 + e$

H_2-to-H transition

$Z=10^{-2}$

H_2-to-H transition

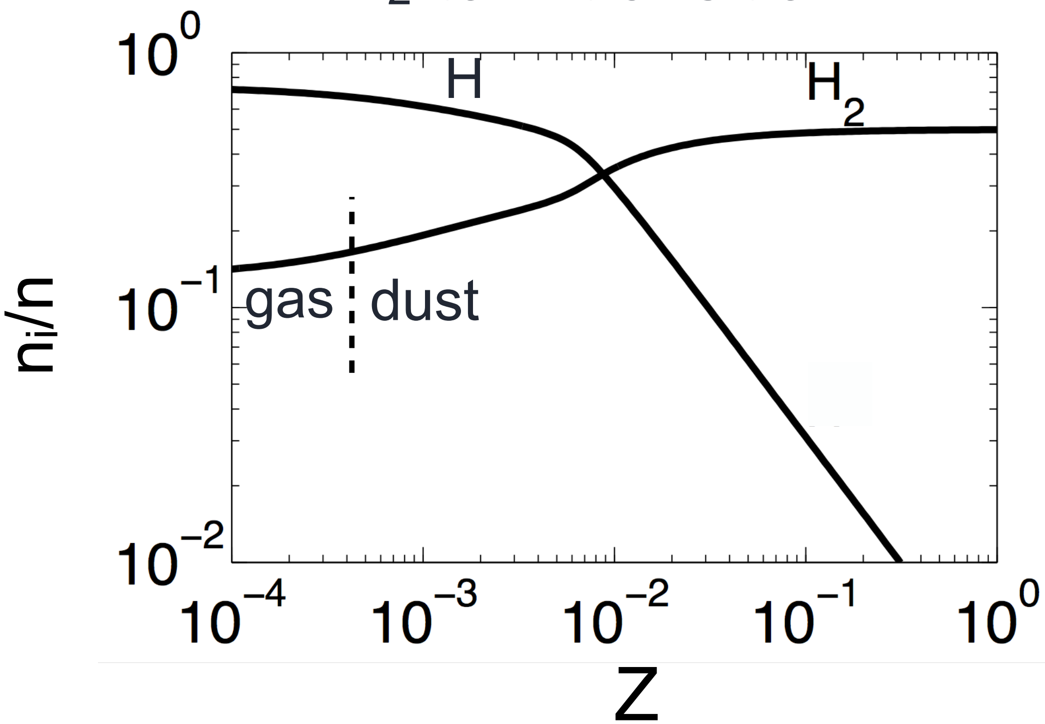

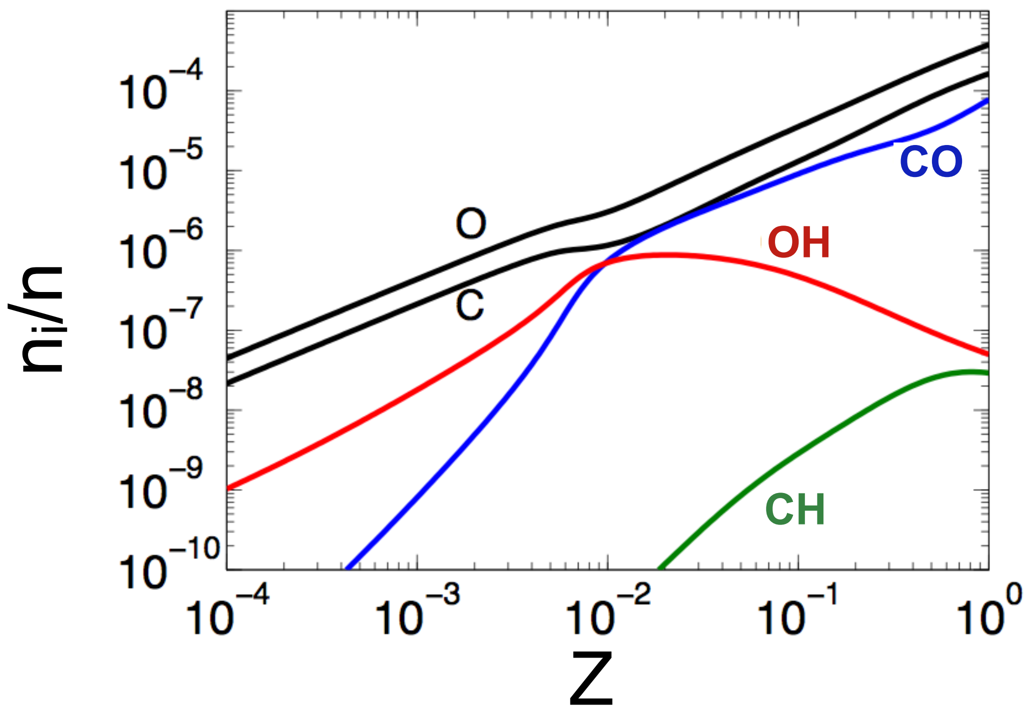

<u>H_2 formation</u>

1. dust grains α Z
2. gas phase

$H + e \rightarrow H^- + \nu$

$H^- + H \rightarrow H_2 + e$

H_2-to-H transition

$Z=10^{-2}$

H_2-to-H transition

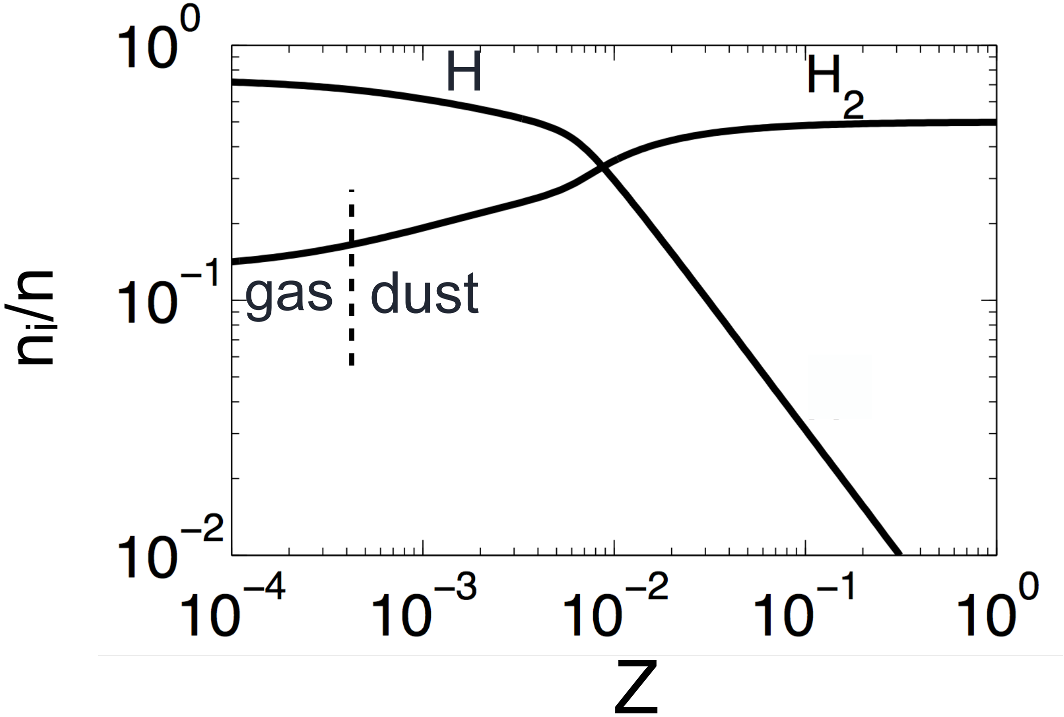

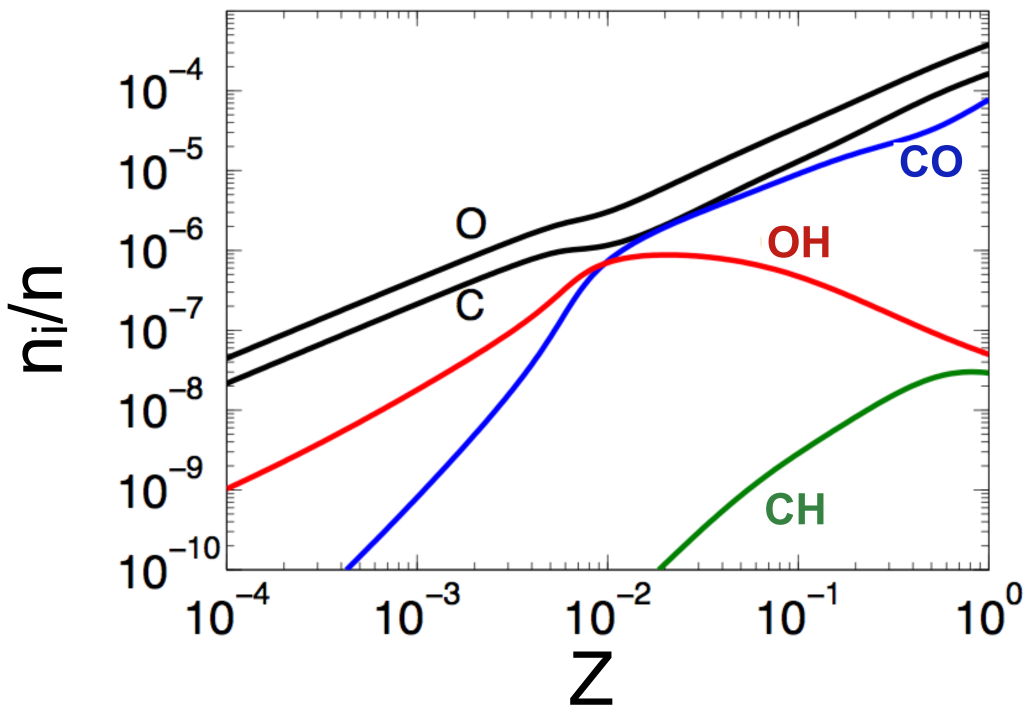

H_2 formation

1. dust grains α Z
2. gas phase

   $H + e \rightarrow H^- + v$

   $H^- + H \rightarrow H_2 + e$

H_2-to-H transition

$Z=10^{-2}$

H_2 regime

CO >> OH, CH

metals α Z

OH α 1/Z

H regime

OH >> CO, CH

CO α Z^2

OH α Z

H_2-to-H transition

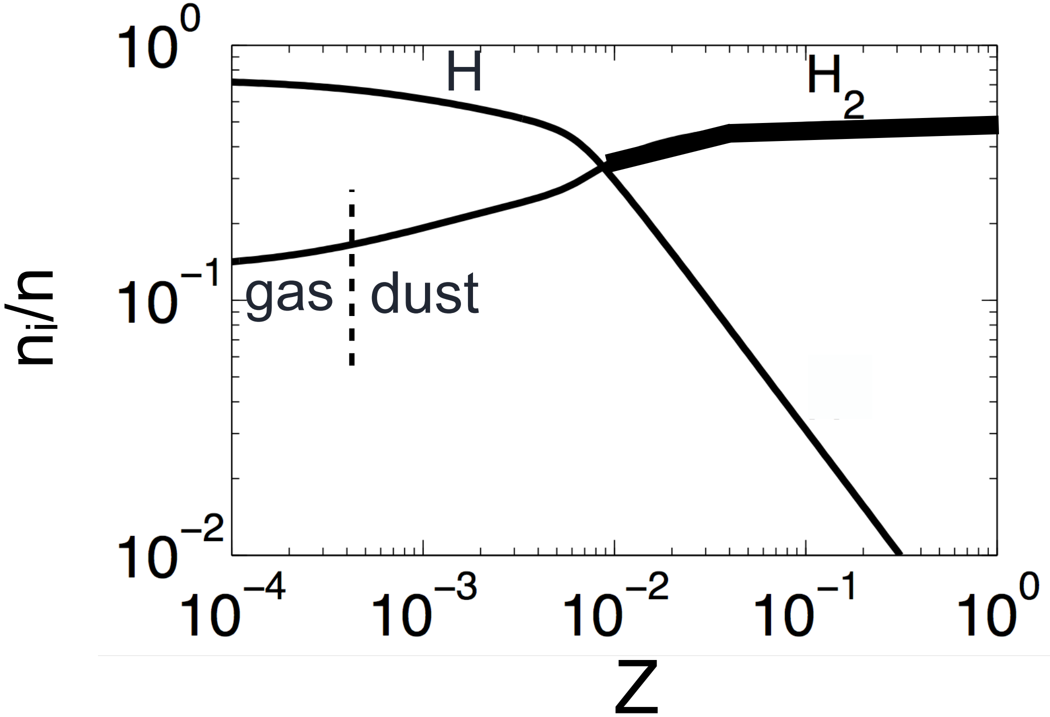

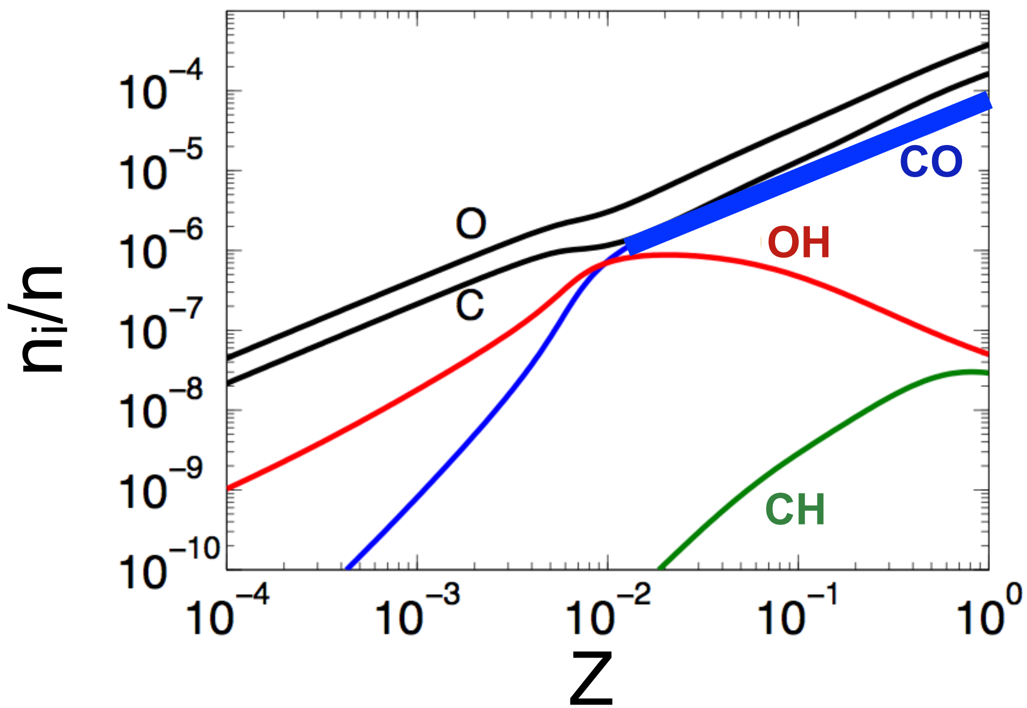

H_2 formation

1. dust grains α Z
2. gas phase

   $H + e \rightarrow H^- + v$

   $H^- + H \rightarrow H_2 + e$

H_2-to-H transition

$Z=10^{-2}$

H_2 regime

CO >> OH, CH

metals α Z

OH α 1/Z

H regime

OH >> CO, CH

CO α Z^2

OH α Z

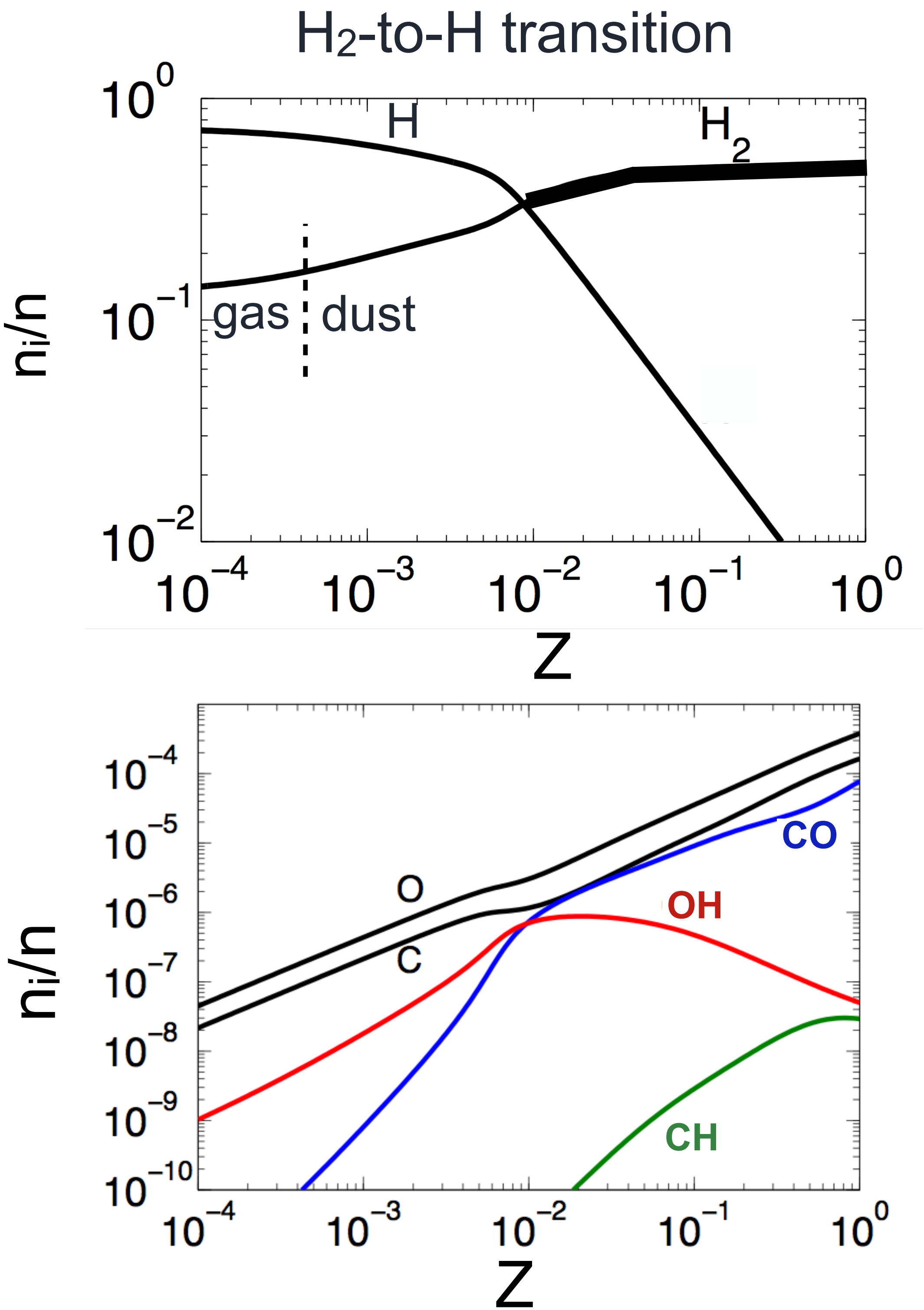

H_2 formation

1. dust grains α Z
2. gas phase
   $H + e \rightarrow H^- + v$
   $H^- + H \rightarrow H_2 + e$

H_2-to-H transition

$Z=10^{-2}$

H_2 regime

CO >> OH, CH

metals α Z

OH α 1/Z

H regime

OH >> CO, CH

CO α Z^2

OH α Z

H_2-to-H transition

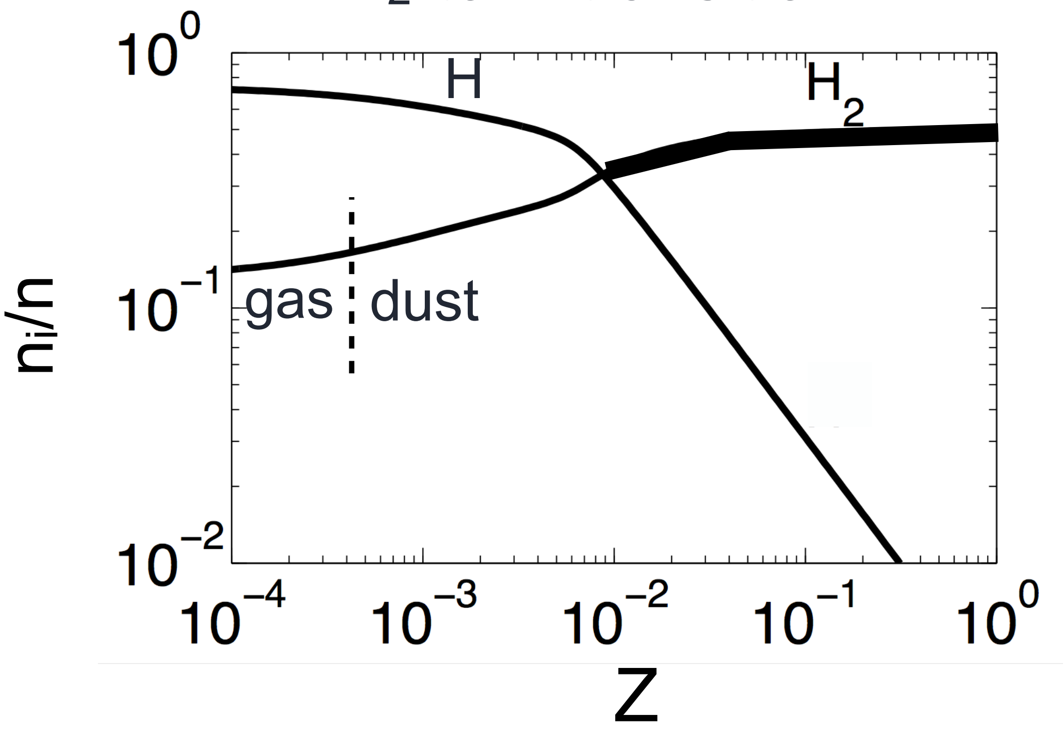

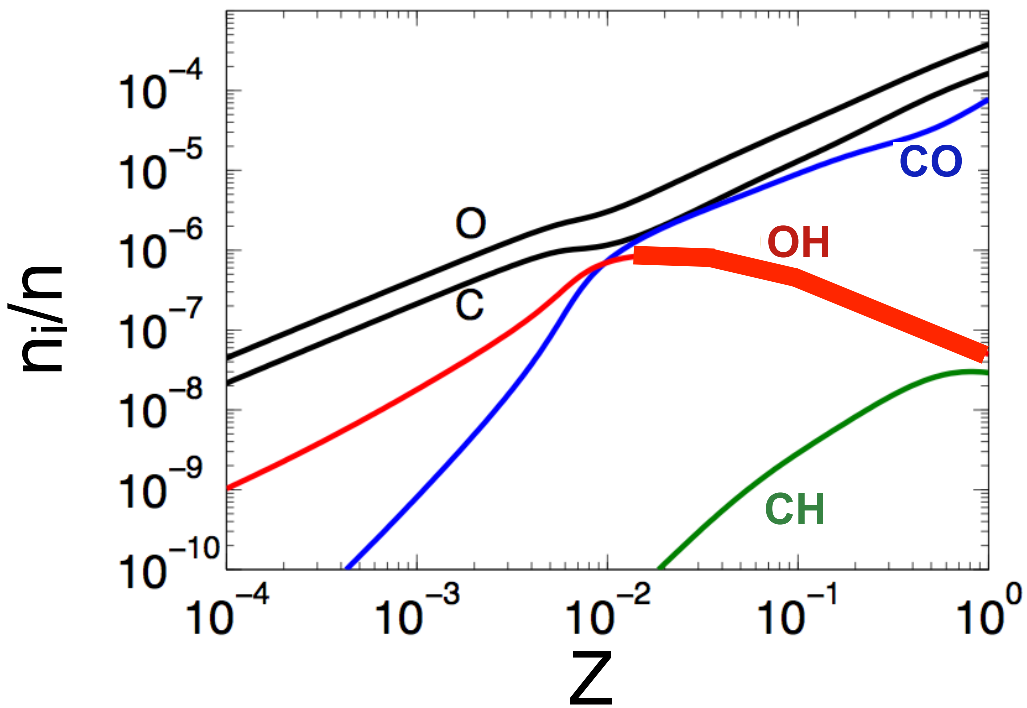

H_2 formation

1. dust grains α Z
2. gas phase

   $H + e \rightarrow H^- + v$

   $H^- + H \rightarrow H_2 + e$

H_2-to-H transition

$Z=10^{-2}$

H_2 regime

CO >> OH, CH

metals α Z

OH α 1/Z

H regime

OH >> CO, CH

CO α Z^2

OH α Z

H_2-to-H transition

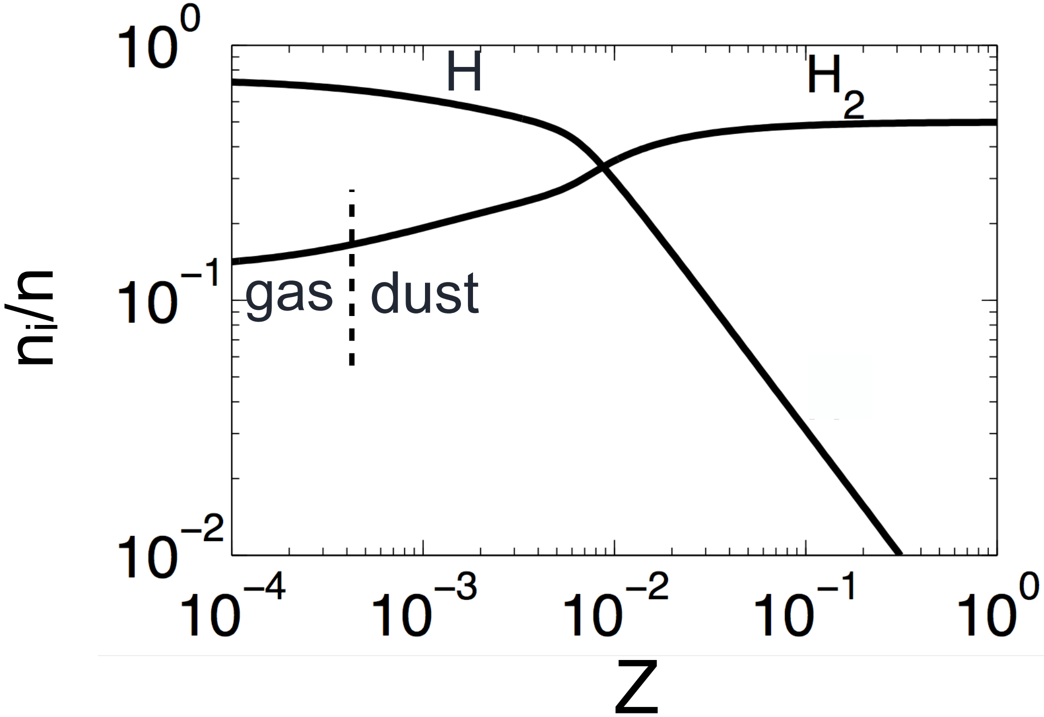

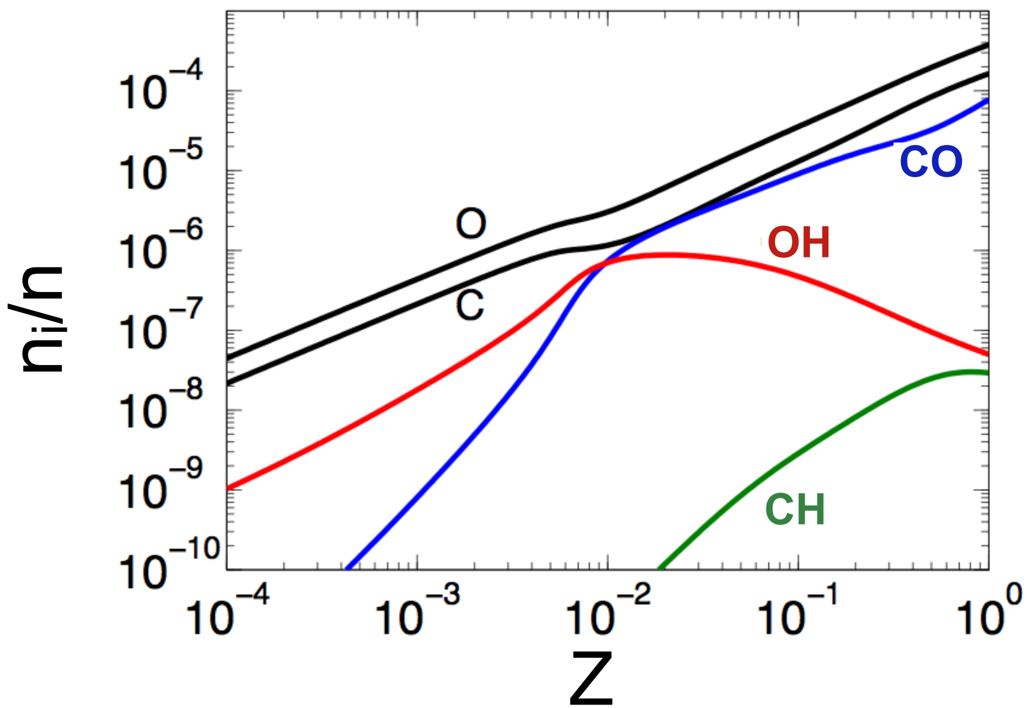

<u>H_2 formation</u>

1. dust grains α Z
2. gas phase

   $H + e \rightarrow H^- + v$

   $H^- + H \rightarrow H_2 + e$

H_2-to-H transition

$Z=10^{-2}$

<u>H_2 regime</u>

CO >> OH, CH

metals α Z

OH α 1/Z

<u>H regime</u>

OH >> CO, CH

CO α Z^2

OH α Z

H_2-to-H transition

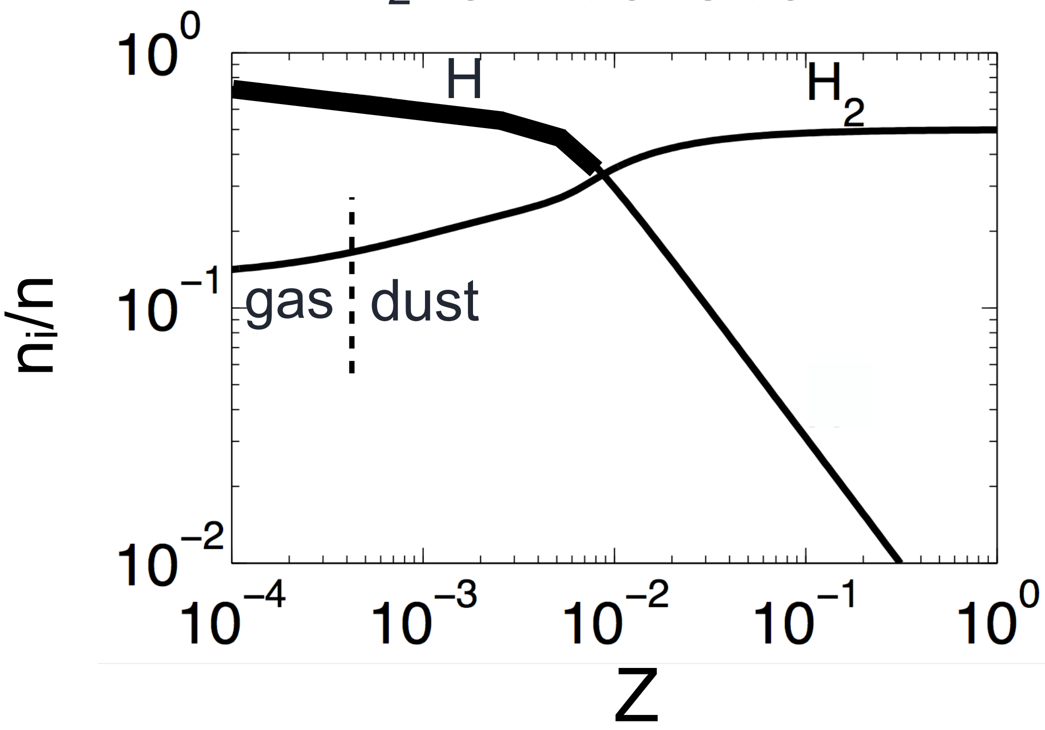

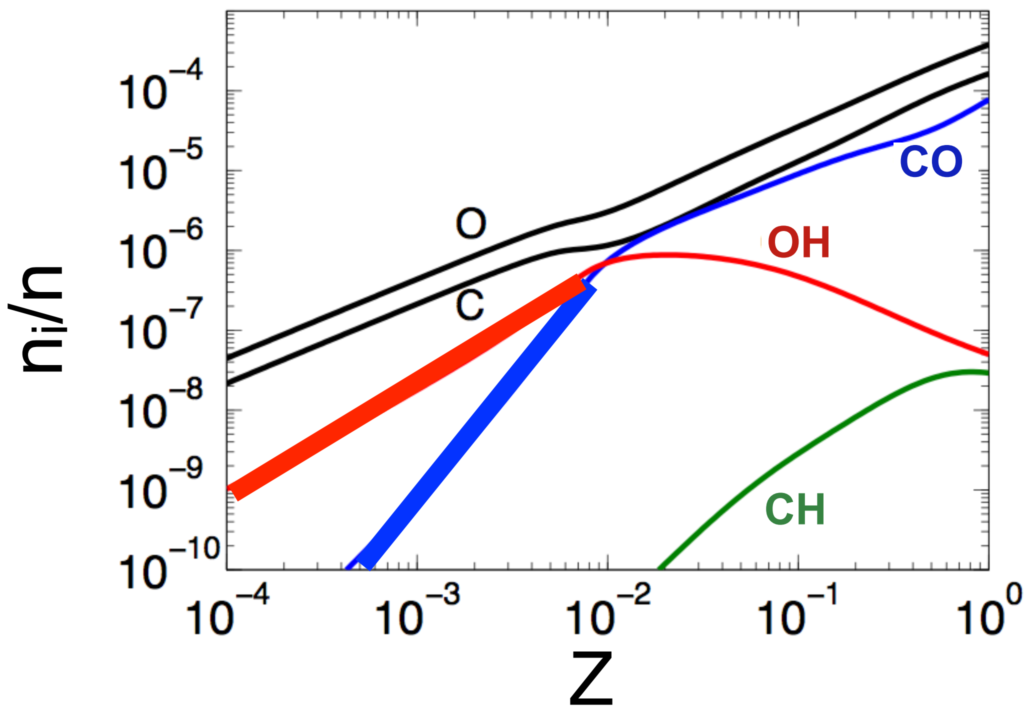

H_2 formation

1. dust grains α Z
2. gas phase

   $H + e \rightarrow H^- + v$

   $H^- + H \rightarrow H_2 + e$

H_2-to-H transition

$Z = 10^{-2}$

H_2 regime

CO >> OH, CH

metals α Z

OH α 1/Z

H regime

OH >> CO, CH

CO α Z^2

OH α Z

H_2-to-H transition

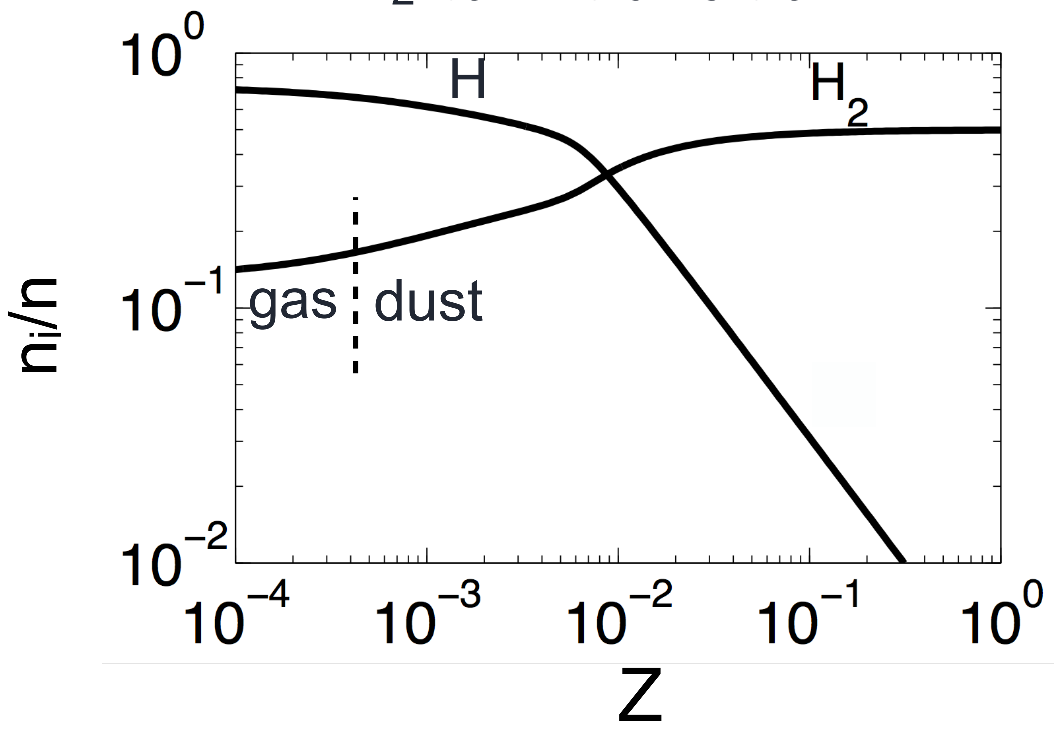

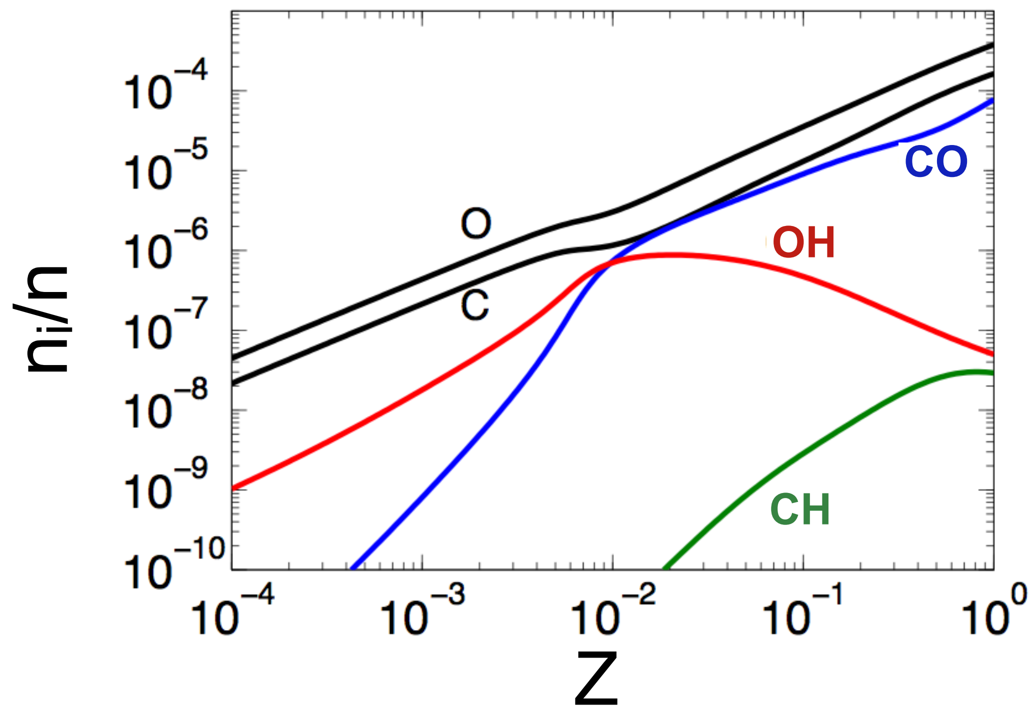

H_2 formation

1. dust grains α Z
2. gas phase

   $H + e \rightarrow H^- + v$

   $H^- + H \rightarrow H_2 + e$

H_2-to-H transition

$Z=10^{-2}$

H_2 regime

CO >> OH, CH

metals α Z

OH α 1/Z

H regime

OH >> CO, CH

CO α Z^2

OH α Z

H_2-to-H transition

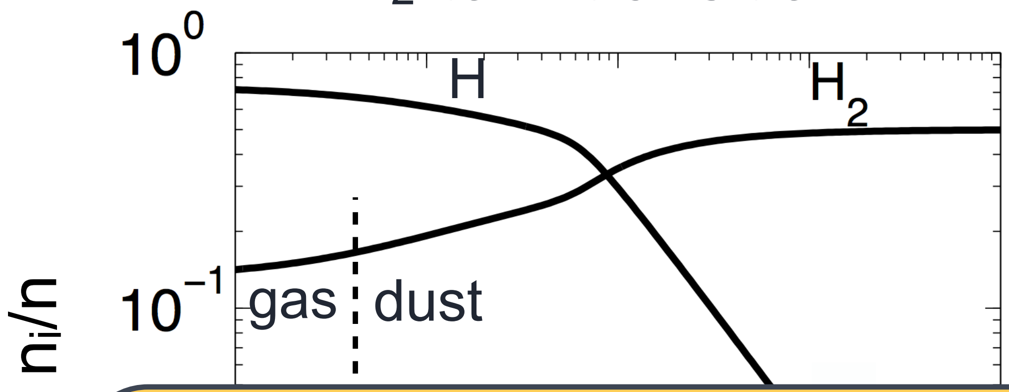

Transition from CO to OH-dominated gas

Correlated with H_2-to-H transition

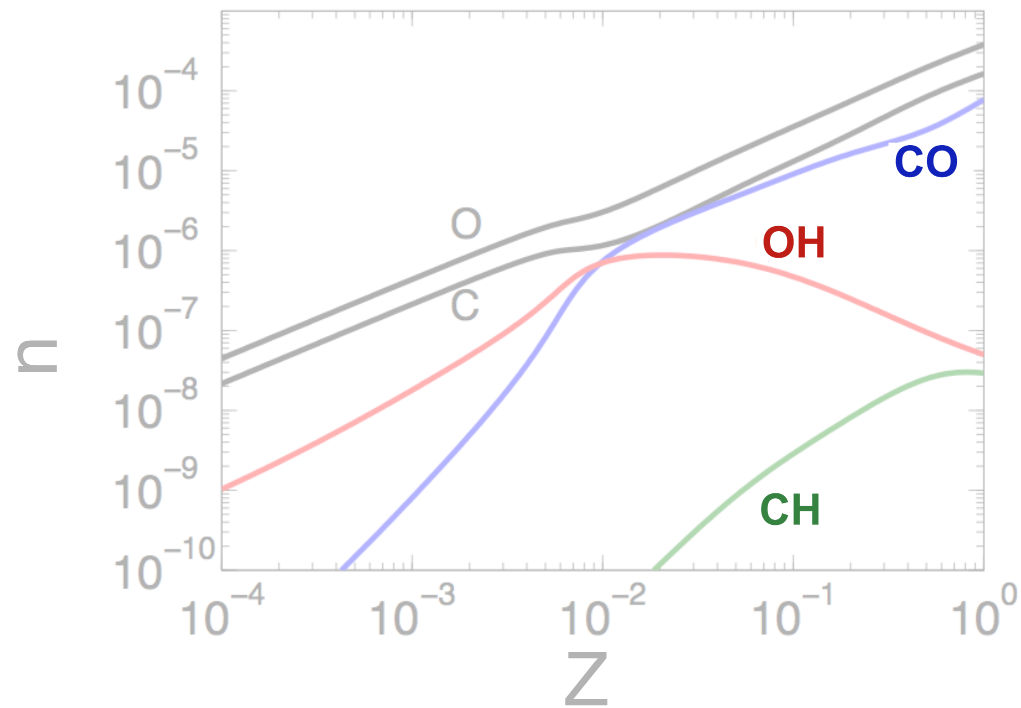

H_2 formation

1. dust grains α Z
2. gas phase

$H + e \rightarrow H^- + v$

$H^- + H \rightarrow H_2 + e$

ansition

0^{-2}

H

CO >> OH, CH

metals α Z

OH α 1/Z

H

OH >> CO, CH

CO

OH α Z

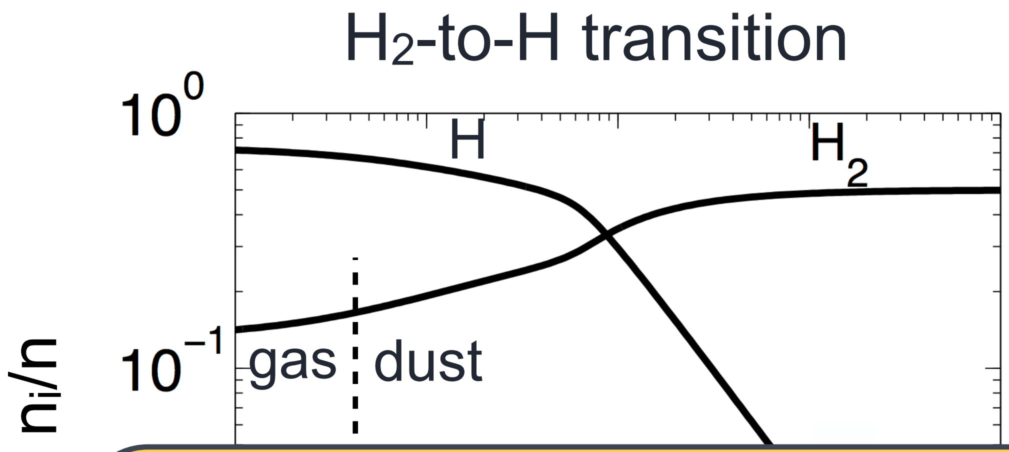

H_2 formation

1. dust grains α Z
2. gas phase
   $H + e \rightarrow H^- + v$
   $H^- + H \rightarrow H_2 + e$

ansition

0^-2

Transition from CO to OH-dominated gas

Correlated with H_2-to-H transition

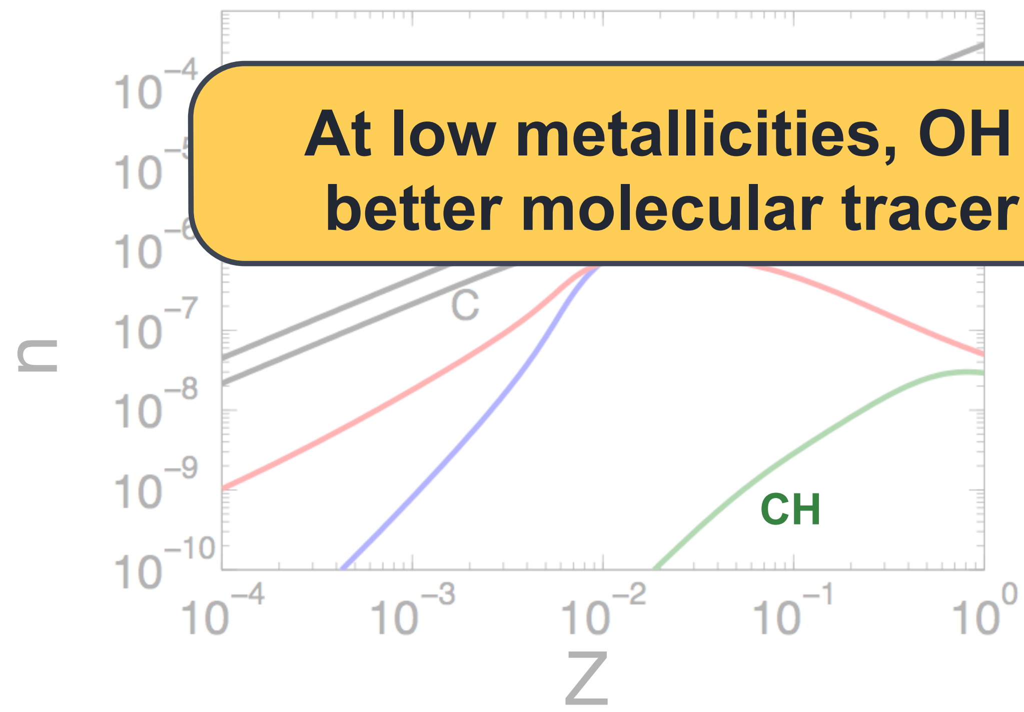

At low metallicities, OH may be a better molecular tracer than CO

\> OH, CH
ls α Z
OH α 1/Z

H
OH >> CO, CH
CO
OH α Z

Thermal Emssion

OH rotational transitions

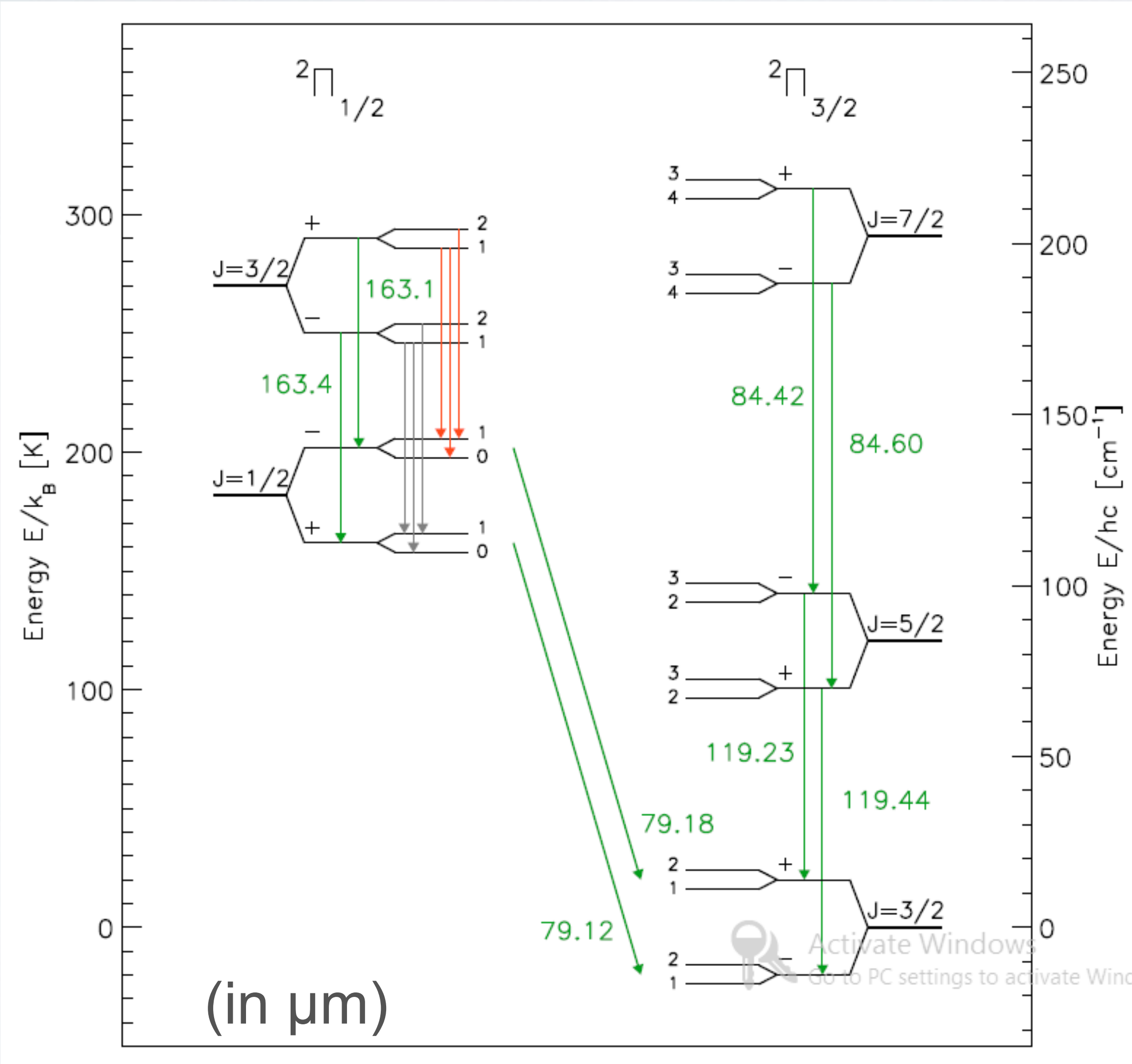

CO ladder

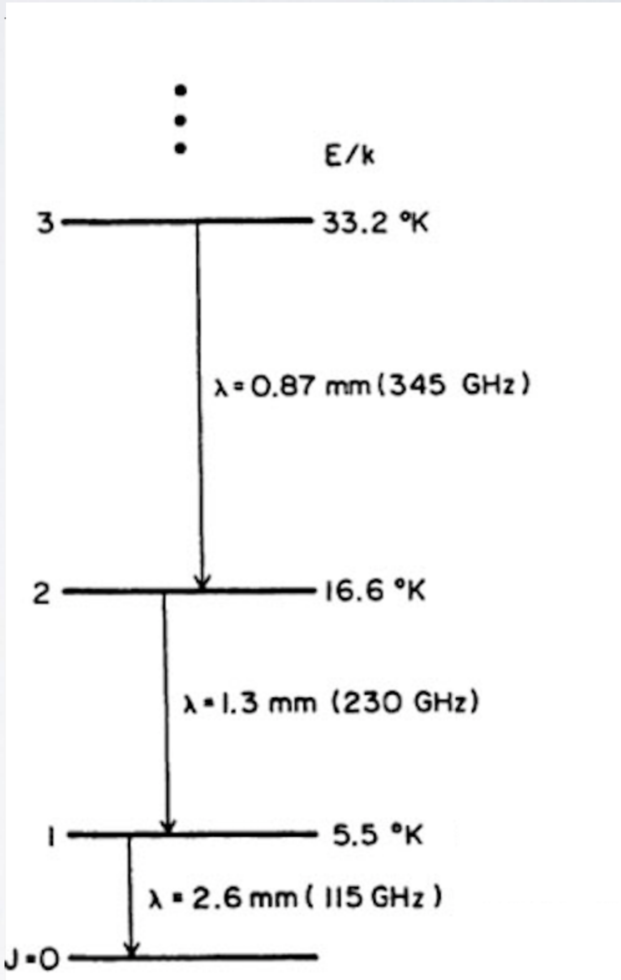

Full 2D Results

H_2/H

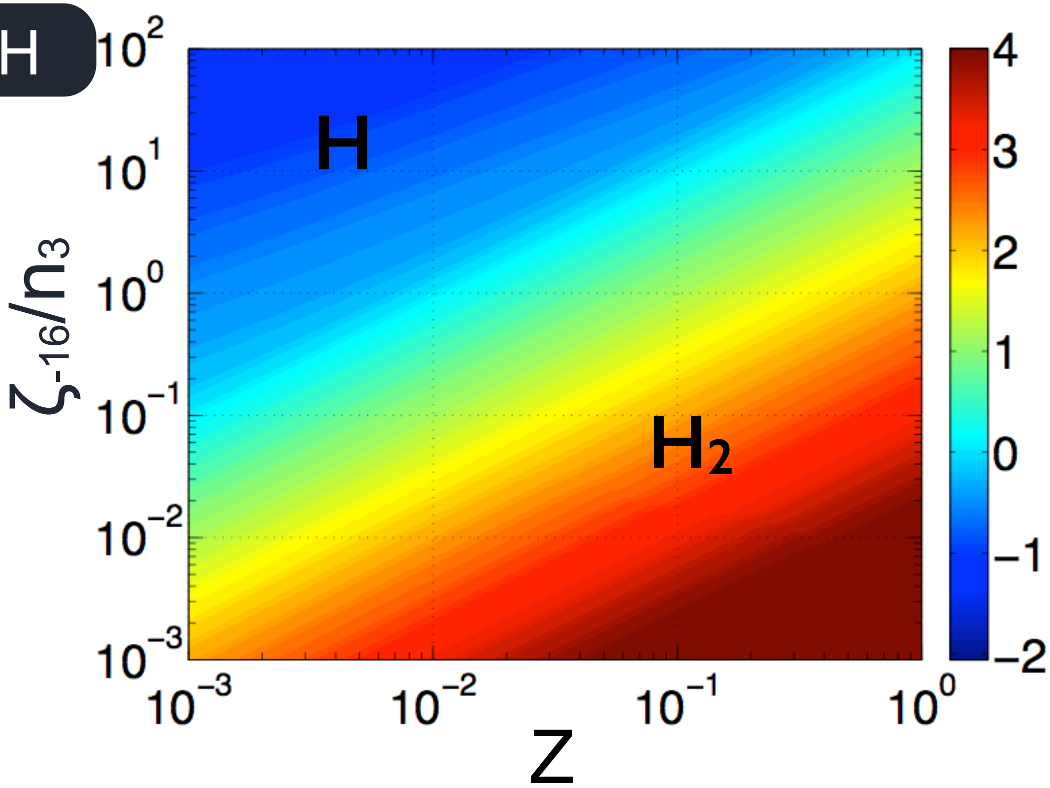

- H_2 formation α nZ
- H_2 removal α ζ

H_2/H

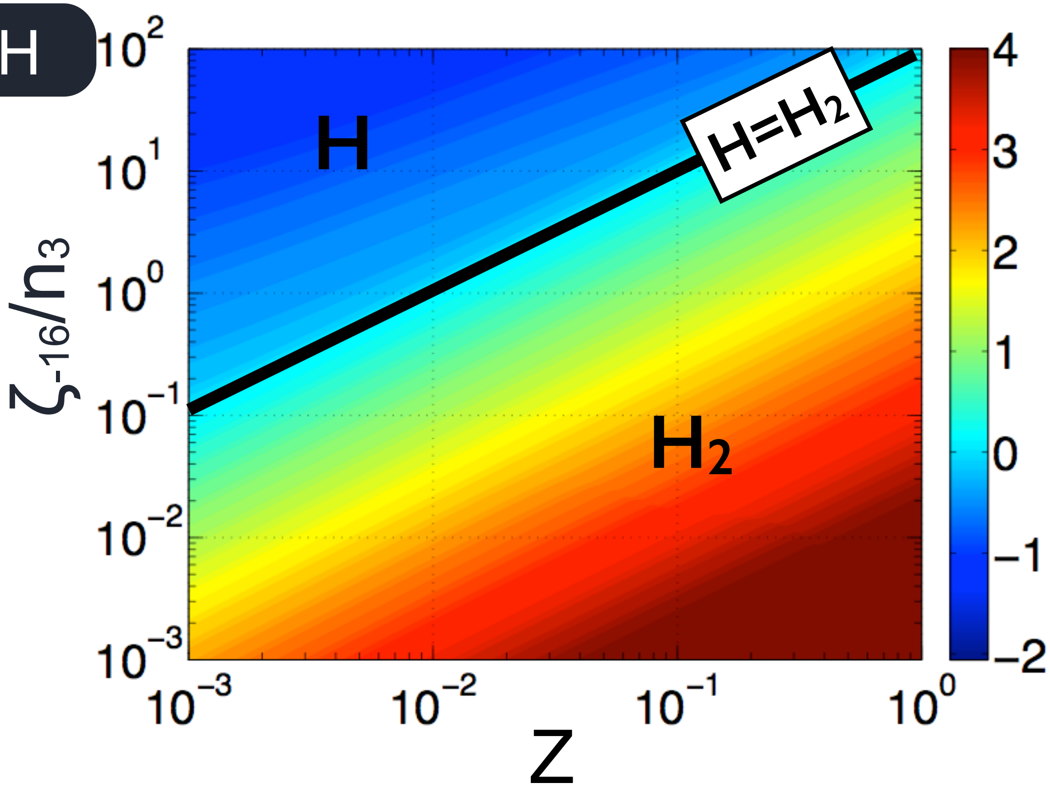

- H_2 formation α nZ
- H_2 removal α ζ

- Transition line:

  $\zeta_{-16}/n_3 \approx 10^2 Z$

H_2/H

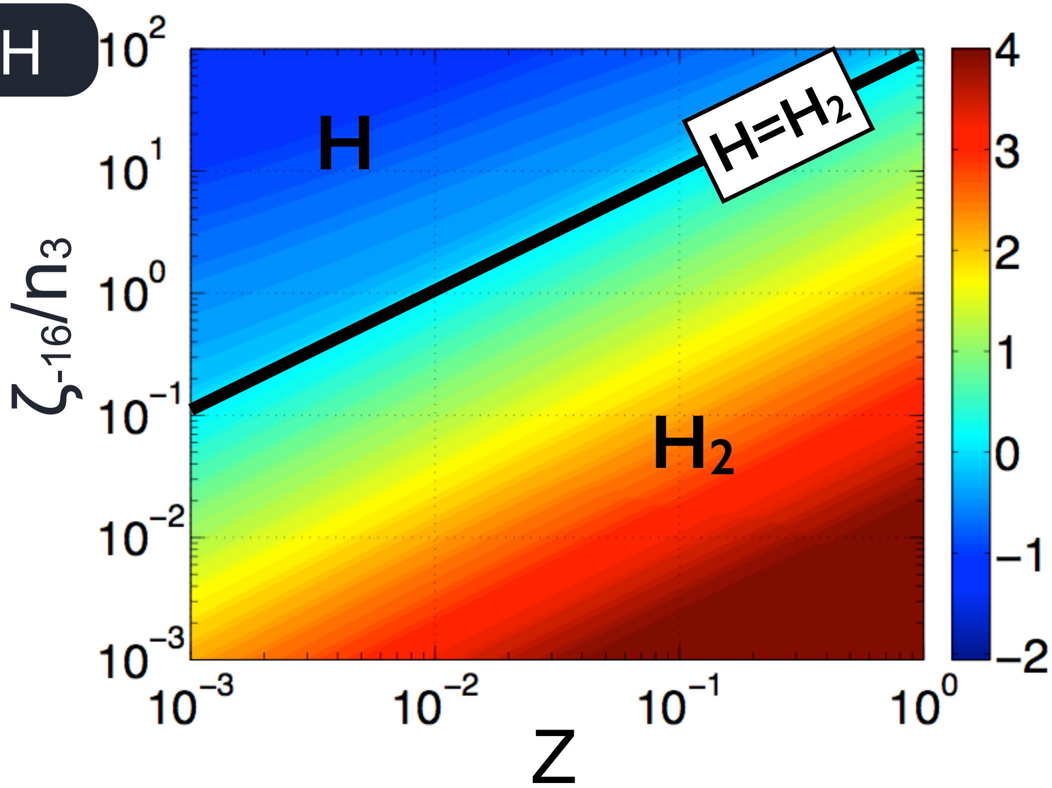

OH/CO

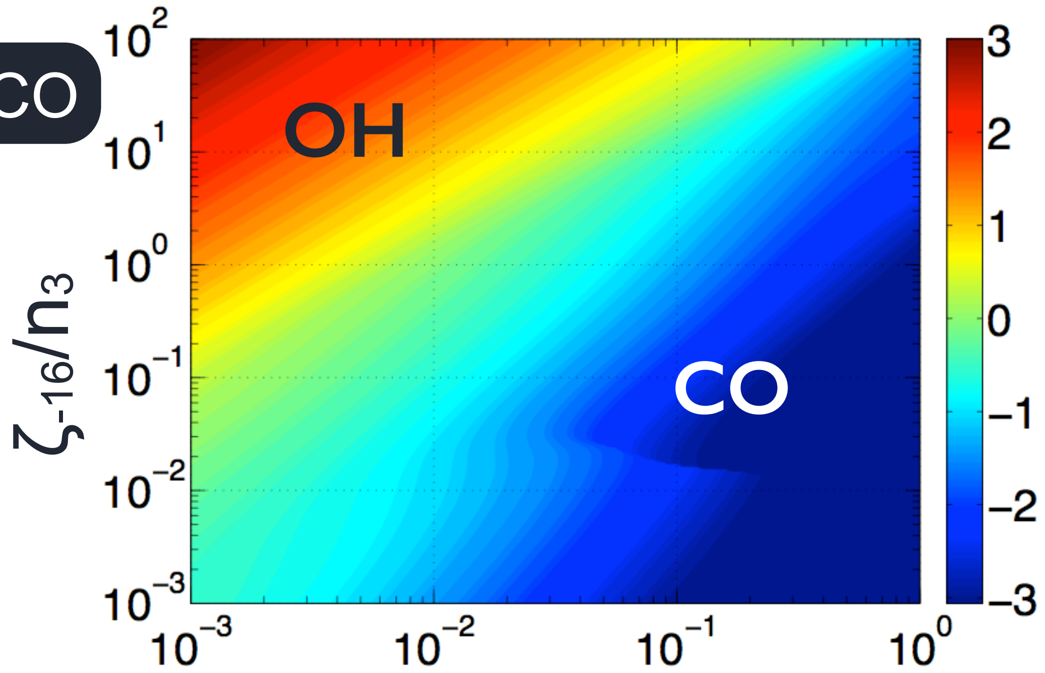

- H_2 formation α nZ
- H_2 removal α ζ

- Transition line:
  $\zeta_{-16}/n_3 \approx 10^2\, Z$

H_2/H

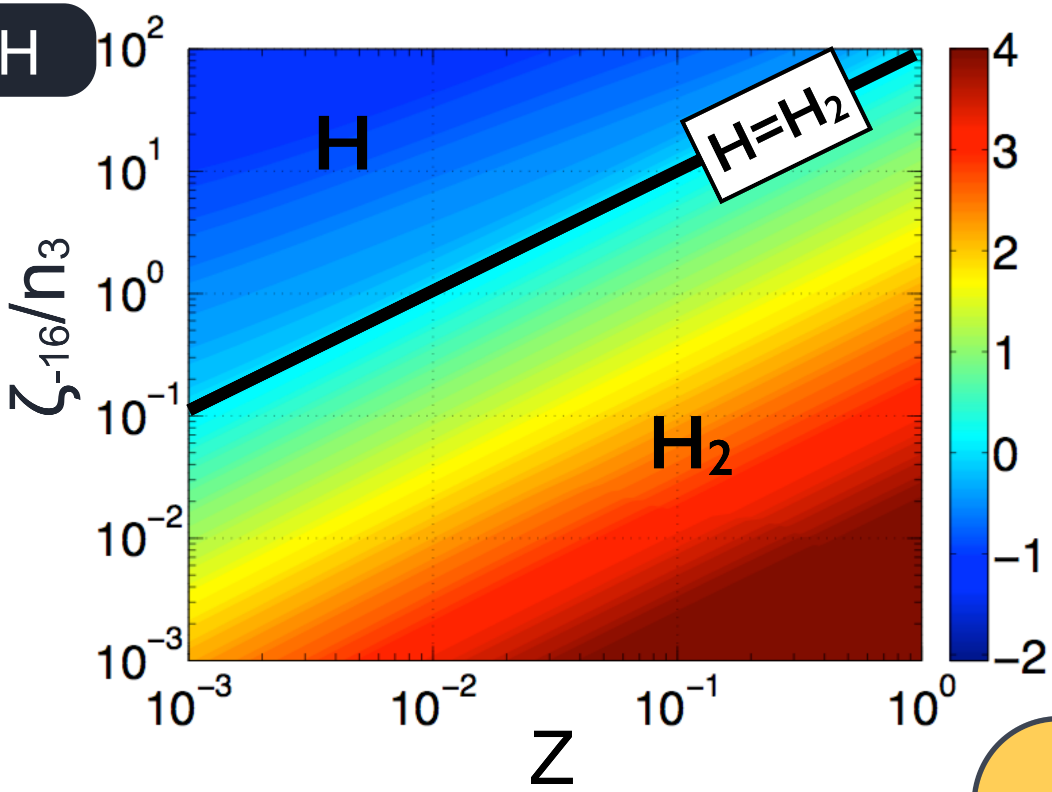

- H_2 formation α nZ
- H_2 removal α ζ

- Transition line:
  $\zeta_{-16}/n_3 \approx 10^2 Z$

OH/CO

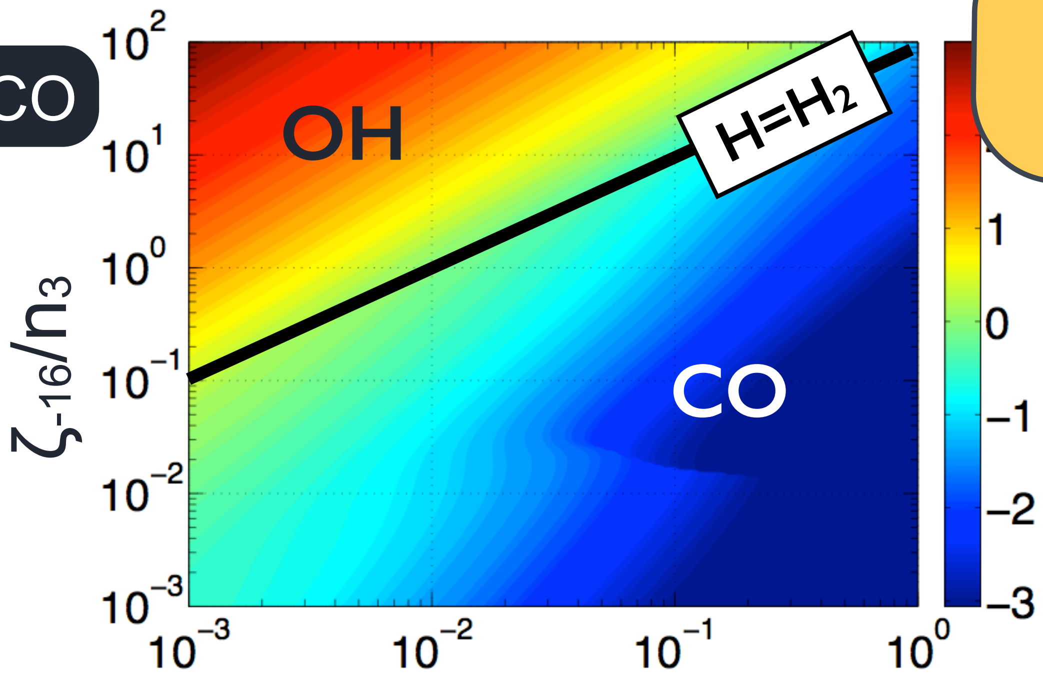

CO-to-OH transition correlated with the H_2-to-H

H_2/H

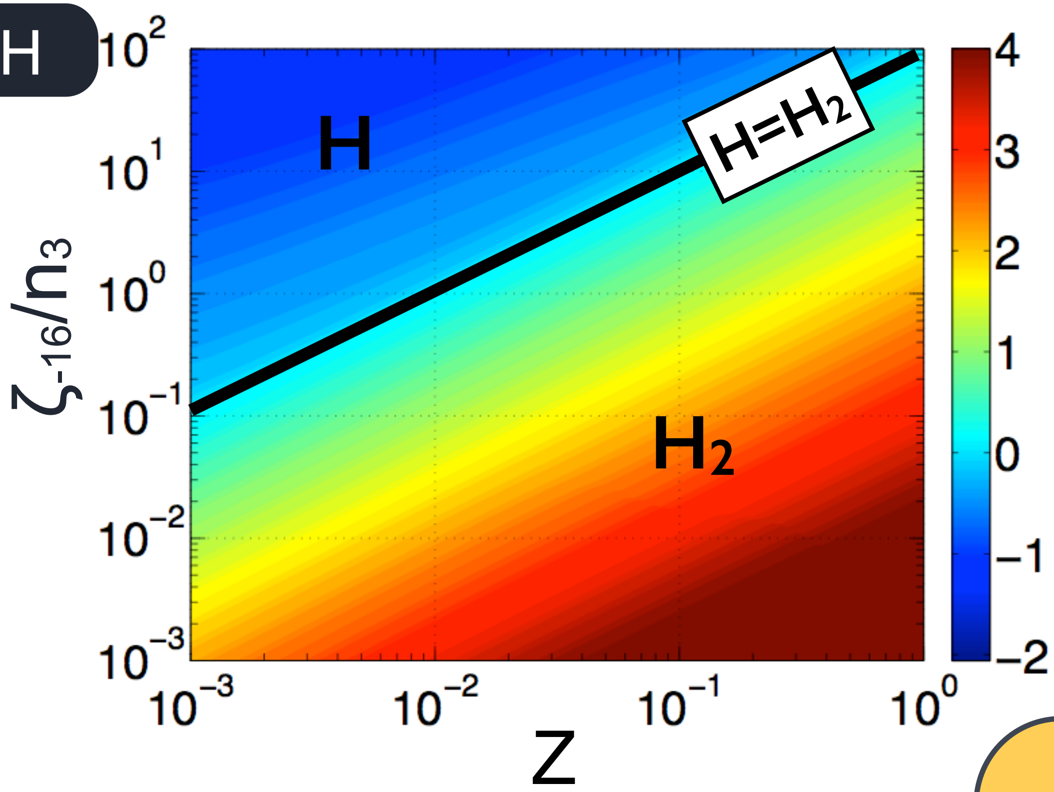

- H_2 formation α nZ
- H_2 removal α ζ

- Transition line:
  $\zeta_{-16}/n_3 \approx 10^2 Z$

OH/CO

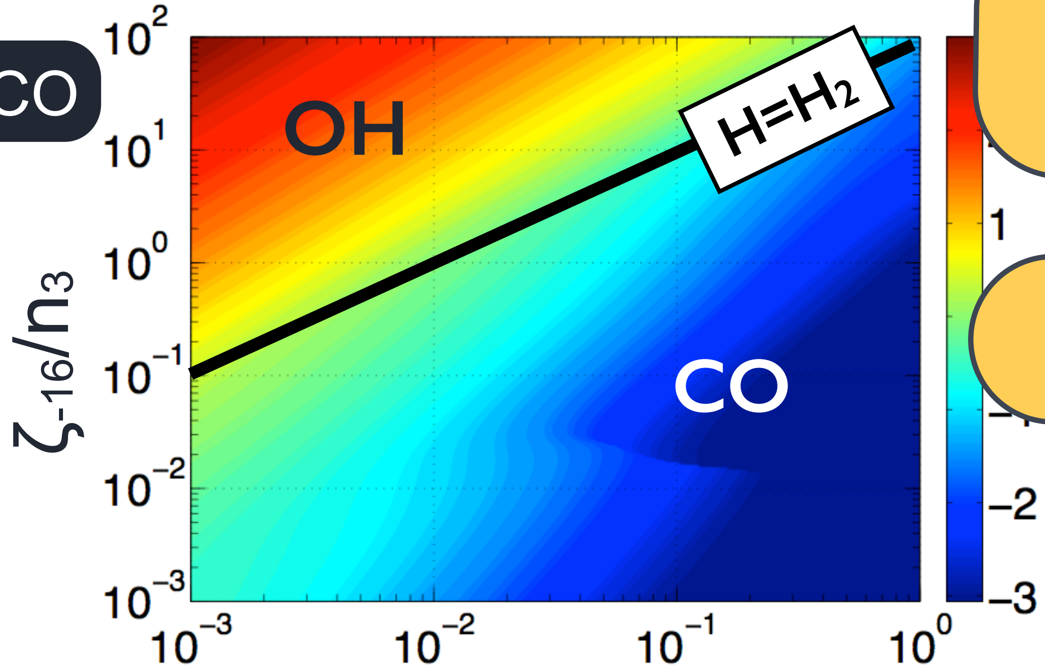

CO-to-OH transition correlated with the H_2-to-H

Insensitive to FUV

H_2/H

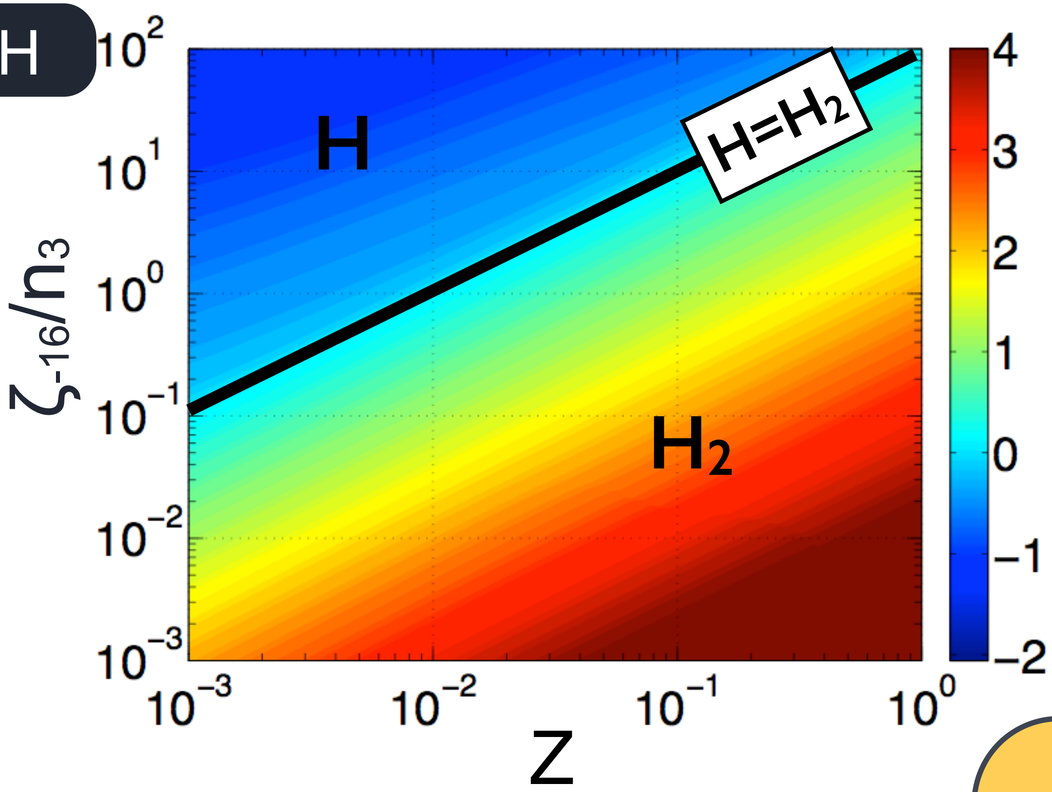

- H_2 formation α nZ
- H_2 removal α ζ

- Transition line:
  $\zeta_{-16}/n_3 \approx 10^2\, Z$

OH/CO

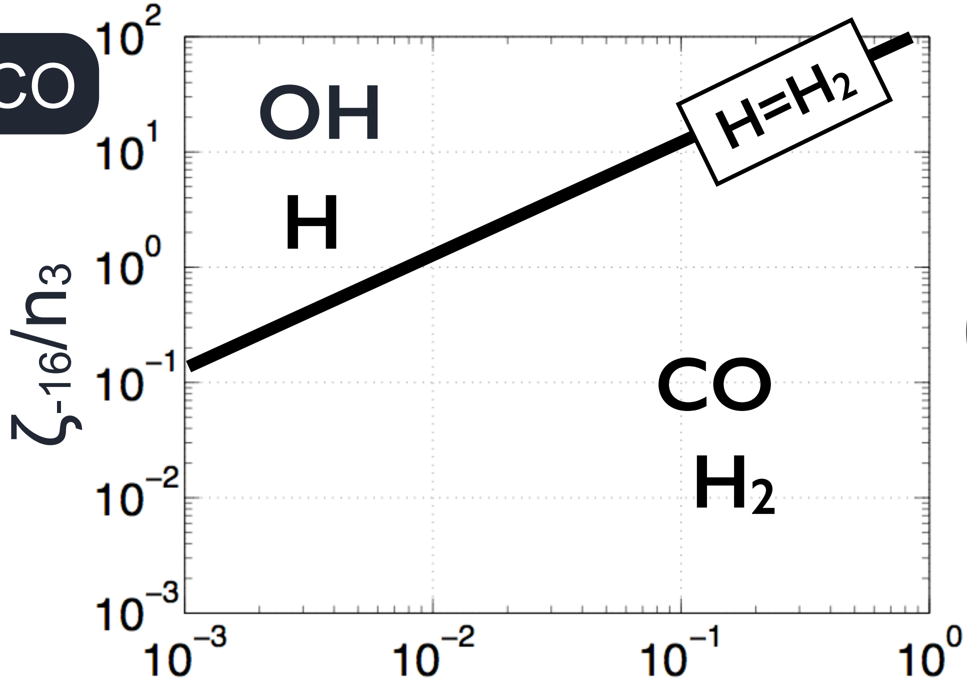

CO-to-OH transition correlated with the H_2-to-H

Insensitive to FUV

CO/H_2 ratio - important for CO optical depth and α_{CO}

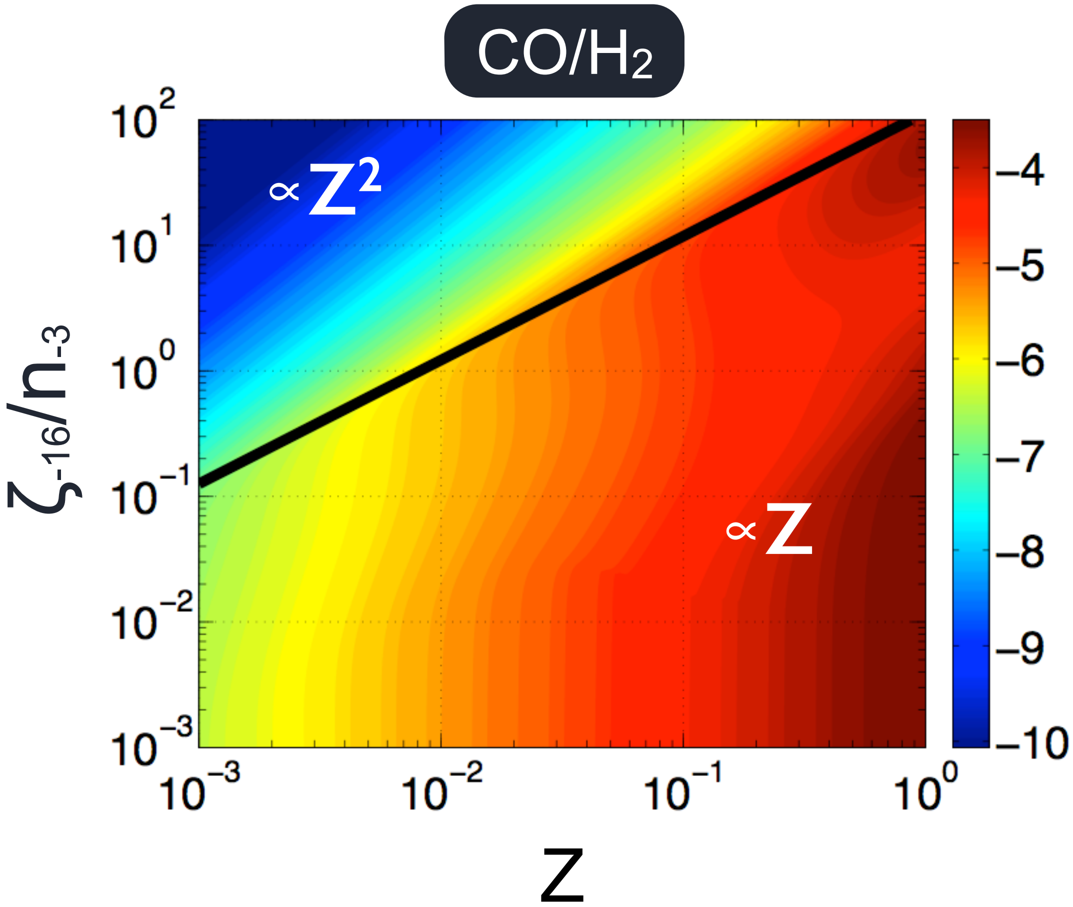

CO/H_2 ratio - important for CO optical depth and α_{CO}

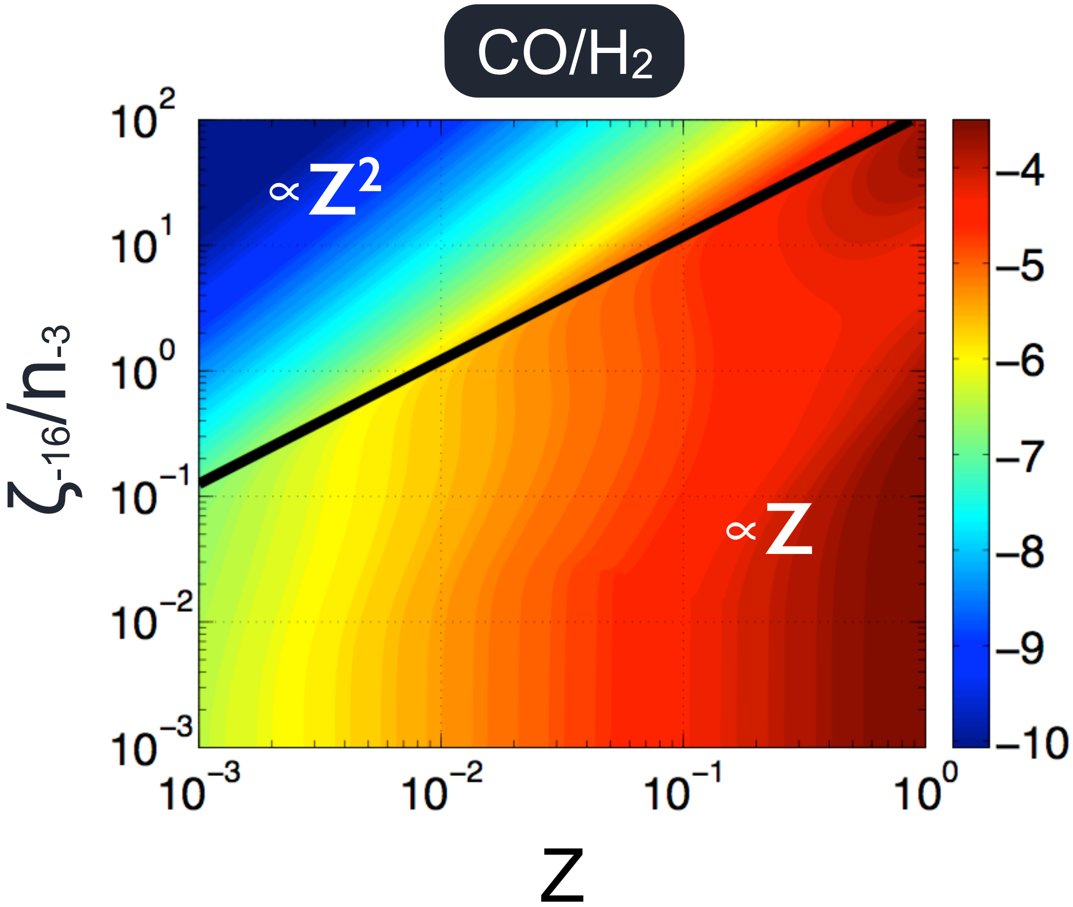

H_2 regime

- CO/H_2 α Z
- A large fraction of the carbon is always locked in CO

CO/H_2 ratio - important for CO optical depth and α_{CO}

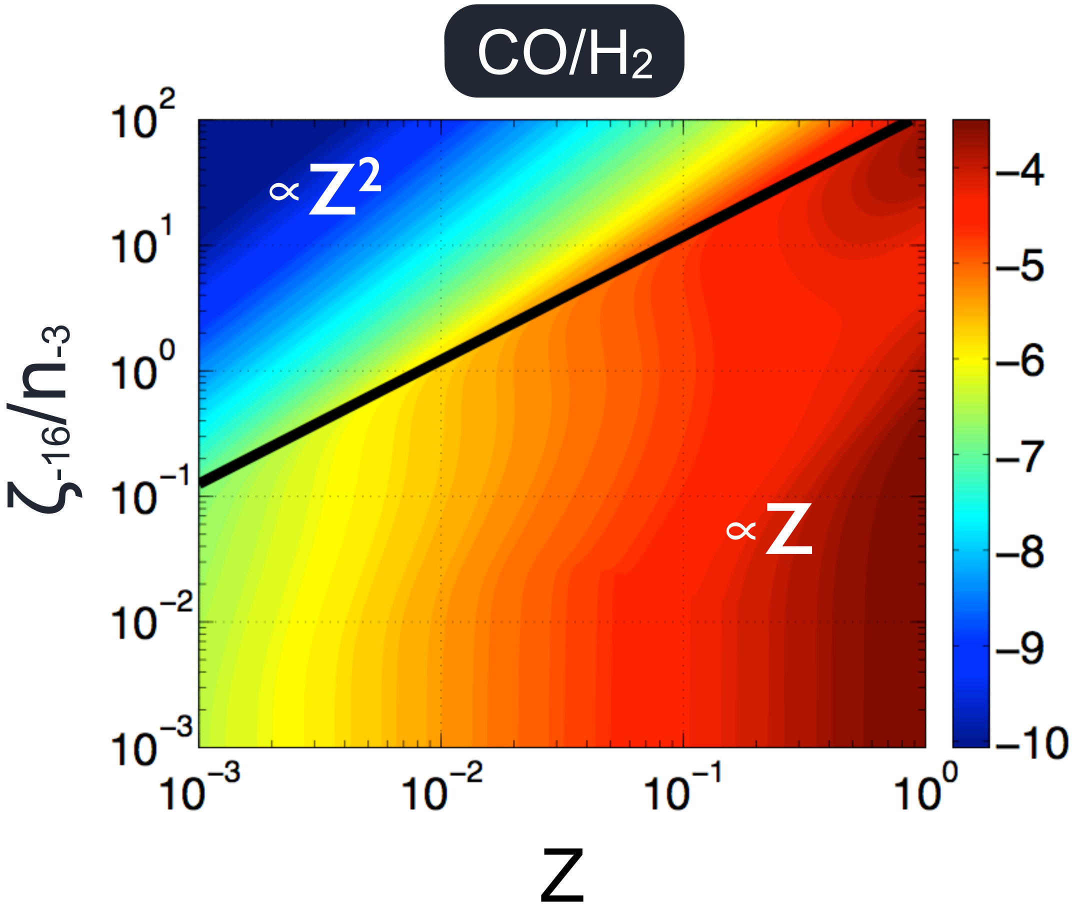

H2 regime

- $CO/H_2 \propto Z$
- A large fraction of the carbon is always locked in CO

H regime

- $CO/H_2 \propto Z^2$
- CO vanishes

Summary

H_2 regime

- CO dominated
- $CO/H_2 \propto Z'$
- A large fraction of the carbon is in CO

H regime

- OH dominated
- $CO/H_2 \propto Z'^2$
- CO vanishes

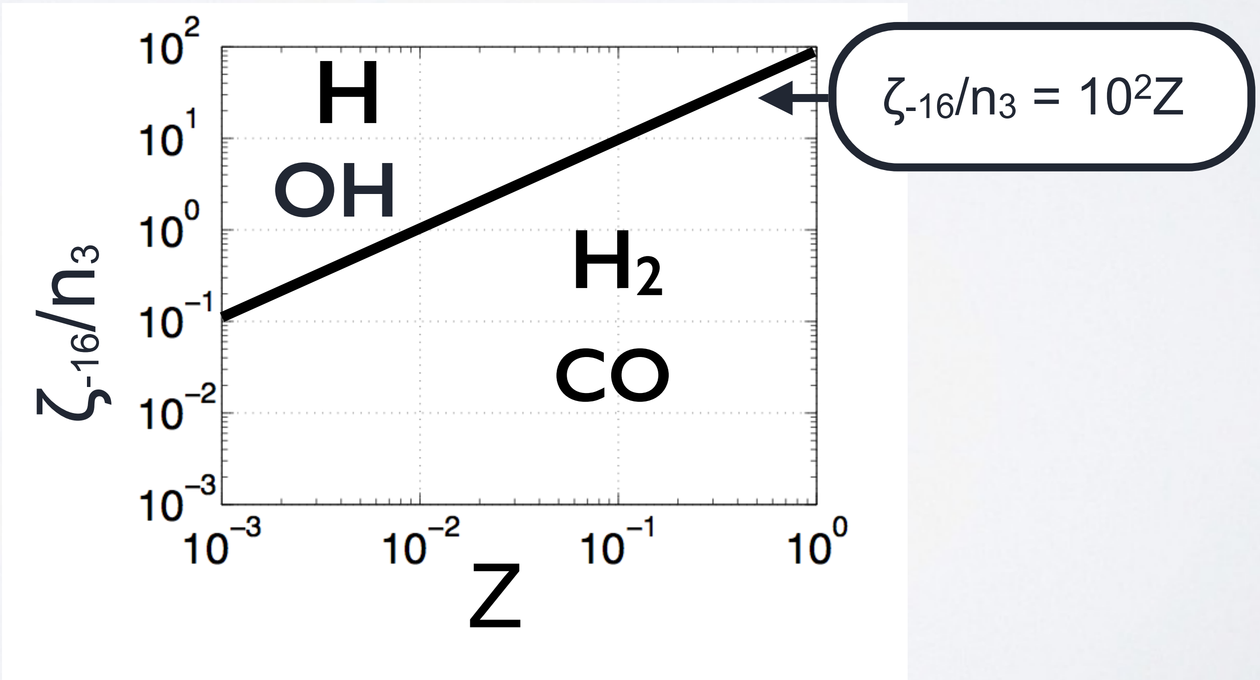

"GMC-like (star-forming) clouds for the Pop-II generation may have been OH-dominated and atomic rather than CO-dominated and molecular."

Bialy & Sternberg

arXiv 1409.6724

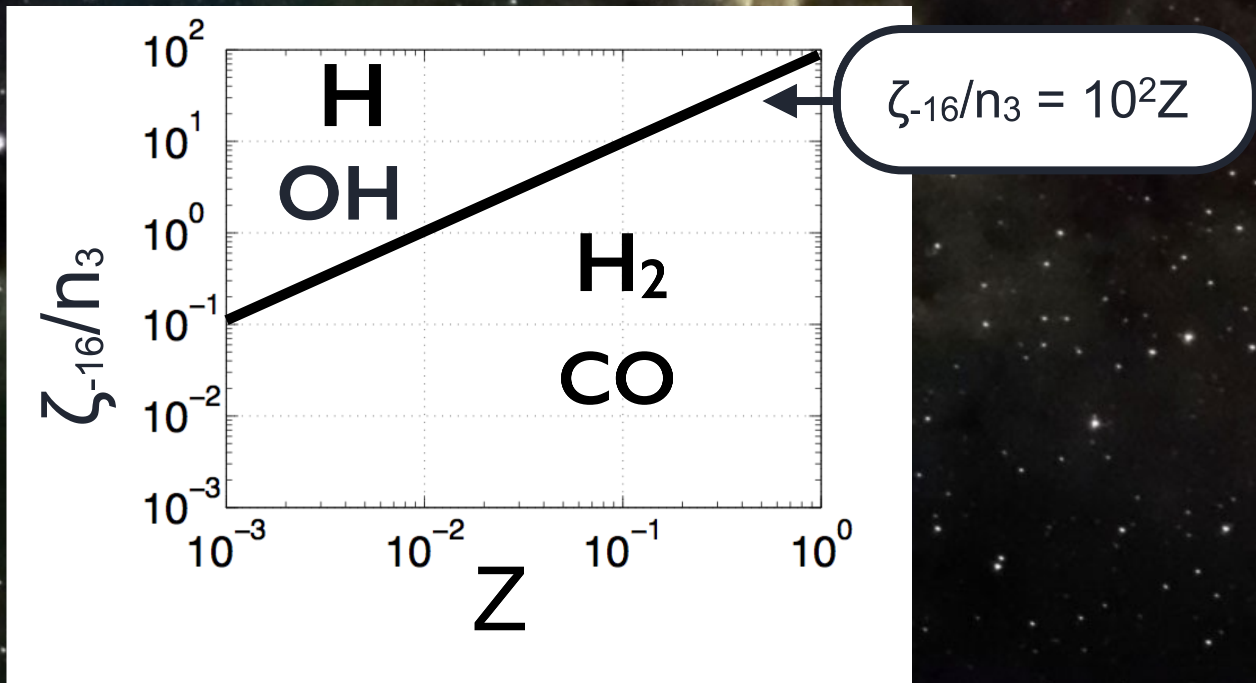

Additional slides

FUV=0

$$\sum_{jl} k_{ijl}(T)\, n_j\, n_l + \zeta \left[\sum_j a^{\rm D}_{ij}\, n_j + x_{\rm H_2} \sum_j a^{\rm P}_{ij}\, n_j \right]$$
$$= n_i \left\{ \sum_{jl} k_{jil}(T)\, n_l + \zeta \left[\sum_j a^{\rm D}_{ji} + x_{\rm H_2} \sum_j a^{\rm P}_{ji} \right] \right\} \quad . \quad (2)$$

$$\sum_{jl} k_{ijl}(T)\, x_j\, x_l + \frac{\zeta}{n} \left[\sum_j a^{\rm D}_{ij}\, x_j + x_{\rm H_2} \sum_j a^{\rm P}_{ij}\, x_j \right]$$
$$= x_i \left\{ \sum_{jl} k_{jil}(T)\, x_l + \frac{\zeta}{n} \left[\sum_j a^{\rm D}_{ji} + x_{\rm H_2} \sum_j a^{\rm P}_{ji} \right] \right\} \quad , \quad (6)$$

FUV=1

$$\sum_{jl} k_{ijl}(T)\, x_j\, x_l + \frac{\zeta}{n} \left[\sum_j a^{\rm D}_{ij}\, x_j + x_{\rm H_2} \sum_j a^{\rm P}_{ij}\, x_j \right]$$
$$+ \frac{I_{\rm UV}}{n} \sum_j b_{ij}\, x_j = x_i \left\{ \sum_{jl} k_{jil}(T)\, x_l \right.$$
$$\left. + \frac{\zeta}{n} \left[\sum_j a^{\rm D}_{ji} + x_{\rm H_2} \sum_j a^{\rm P}_{ji} \right] + \frac{I_{\rm UV}}{n} \sum_j b_{ji} \right\} \quad .$$

carbon network

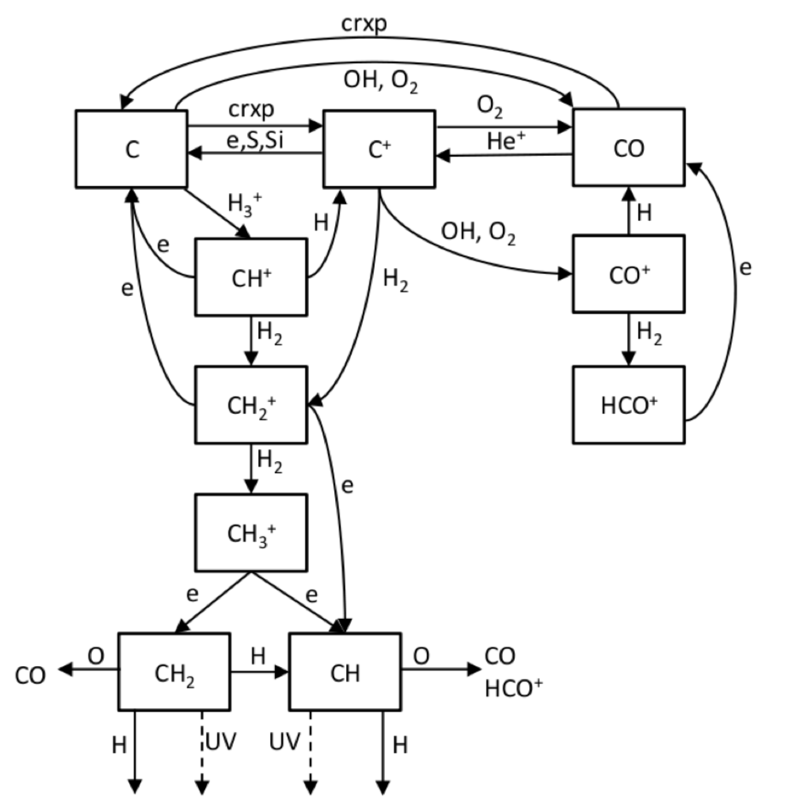

Figure 3. Formation-destruction pathways for CH and CO.

Additional slides

FUV=1

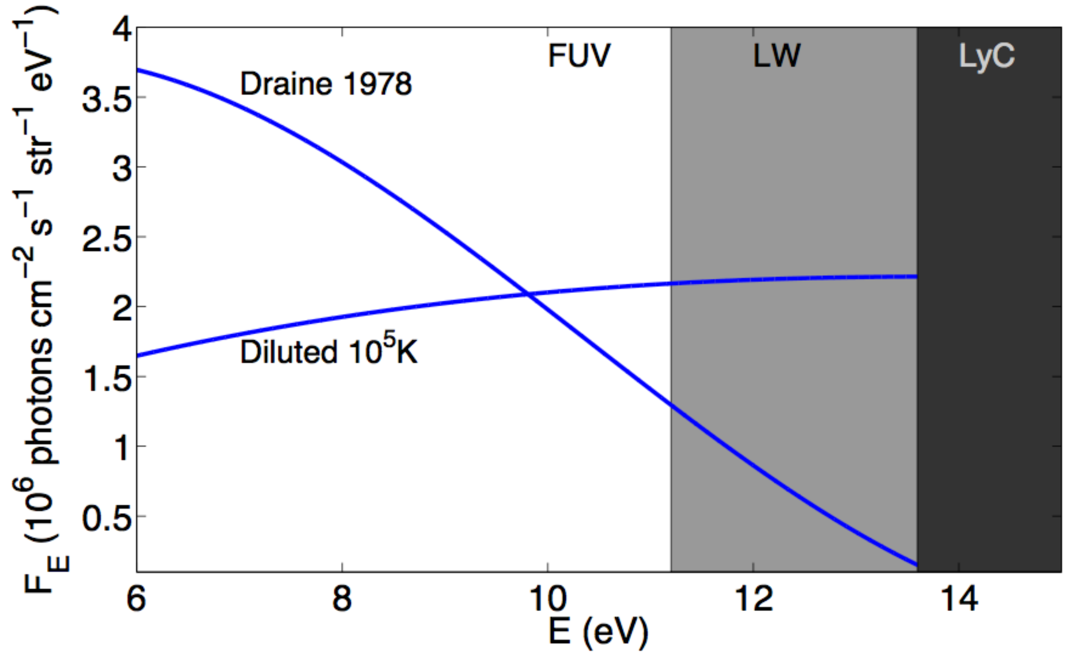

JV spectrum and our diluted 10^5 K black-body
$I_{UV} = 1$ (see text). The light shaded region is the

Table 2. Photorates for $I_{\rm UV} = 1$

Reaction	Threshold (eV)	Photorate Γ (10^{-10} s^{-1})			
		Draine		Diluted 10^5 K	
		thin	LW-blocked	thin	LW-blocked
$OH + \nu \rightarrow O + H$	6.4	3.8	2.8	4.7	2.5
$H_2O + \nu \rightarrow O + H_2$	9.5	0.49	0.28	1.1	0.32
$H_2O + \nu \rightarrow OH + H$	6.0	7.5	5.5	11.7	4.8
$O_2 + \nu \rightarrow O + O$	7.0	7.9	7.0	9.4	5.1
$CH + \nu \rightarrow C + H$	3.4	9.0	8.8	5.5	4.7
$CO + \nu \rightarrow C + O$	11.5[a]	2.6	0.0	14.2	0.0
$C + \nu \rightarrow C^+ + e$	11.3	3.2	0.0	10.1	0.0
$CH + \nu \rightarrow CH^+ + e$	3.4	7.7	0.97	21.3	1.4
$H^- + \nu \rightarrow H + e$	0.75[b]	145.2	145.1	23.1	20.7

[a] CO photodissociation occurs via absorption-line predissociation (Visser, van Dishoeck & Black 2009) and 11.5 eV is the lowest photon energy in this multiline process.
[b] In computing the photodeatachment rate we adopt the normalized Draine and diluted 10^5 K photon intensities from 13.6 eV all the way to the H^- electron detachment threshold of 0.75 eV.

Dependence on dust-to-gas ratio

H/H_2

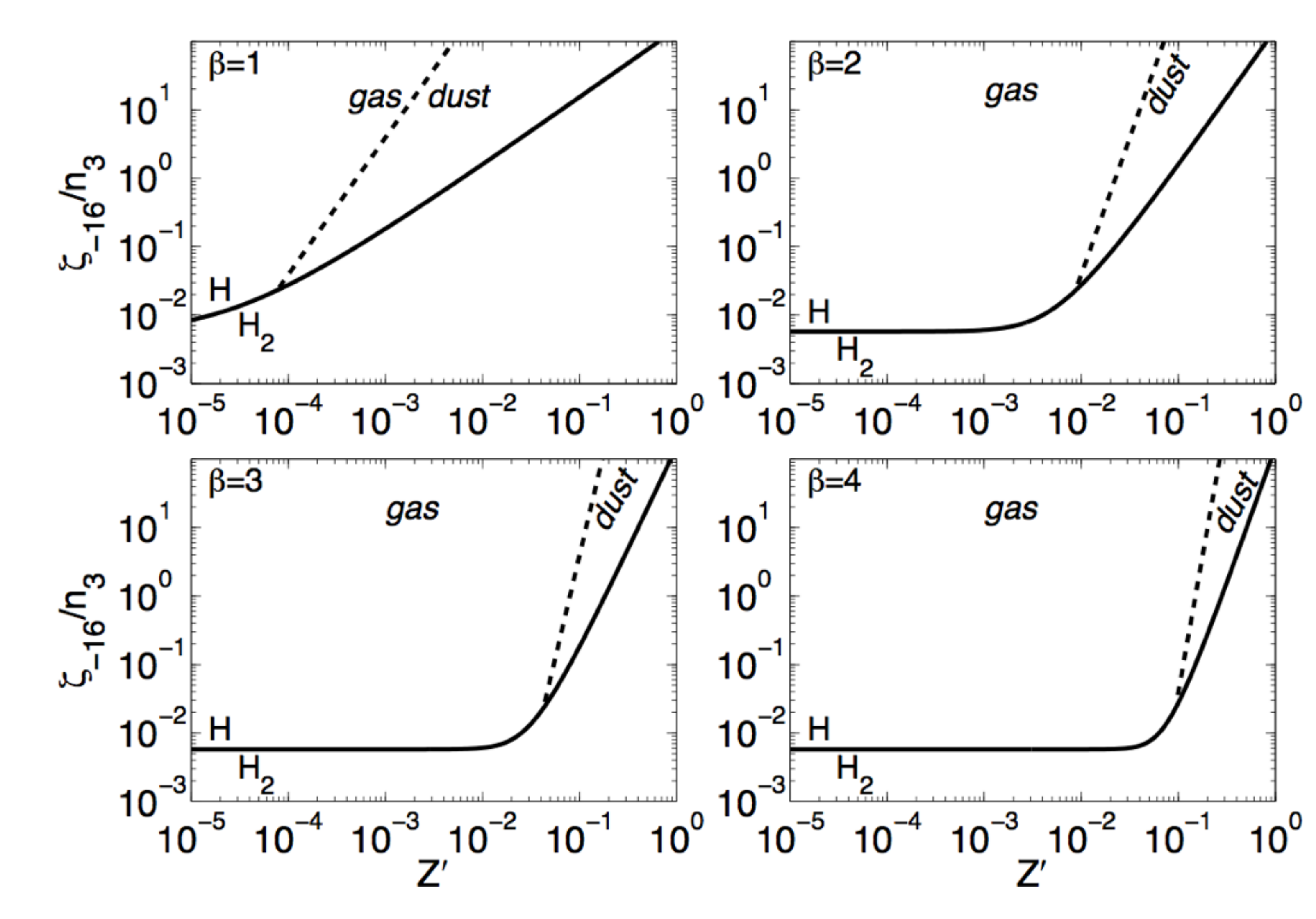

Dependence on Z

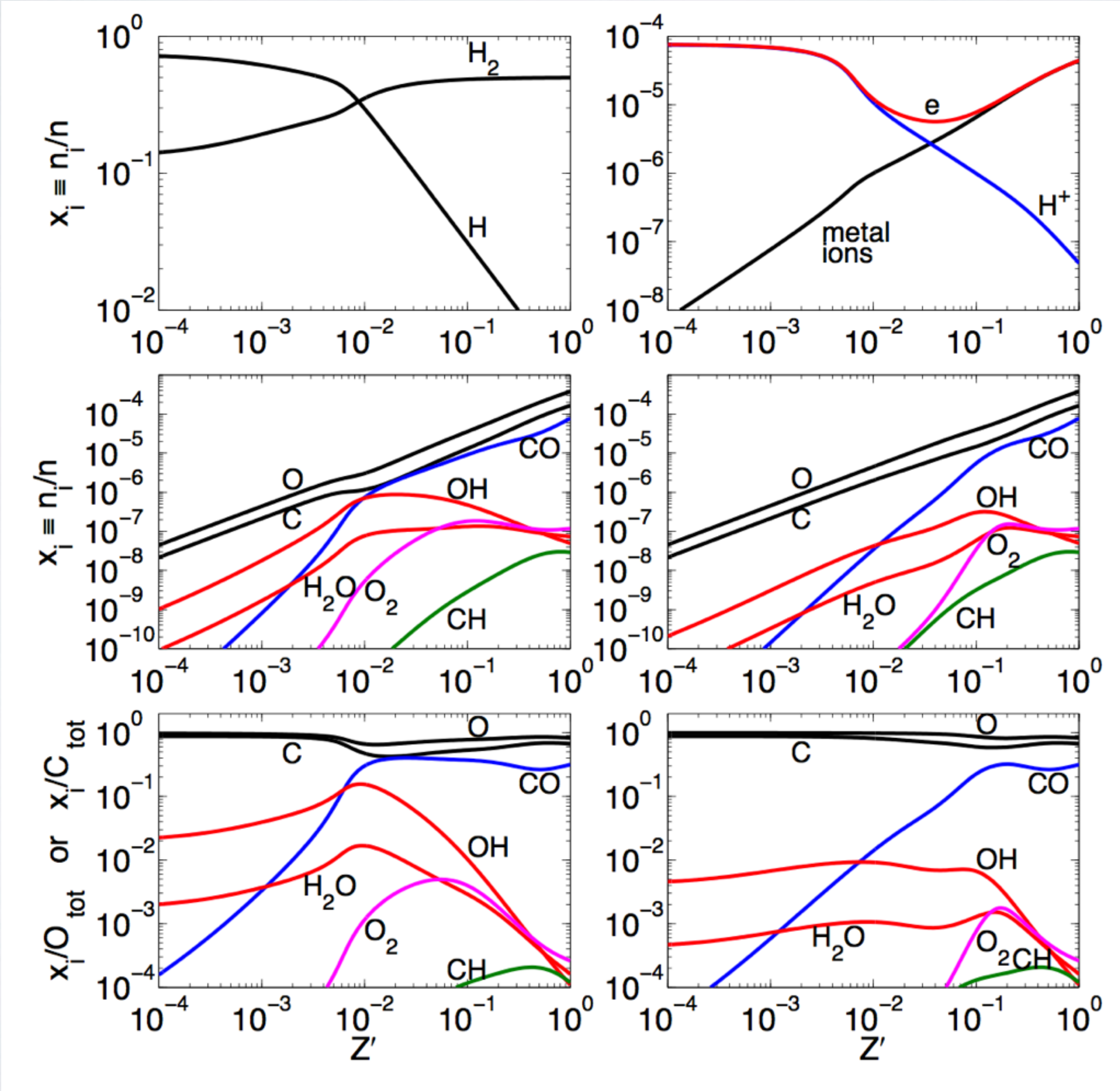

Dependence on ζ/n

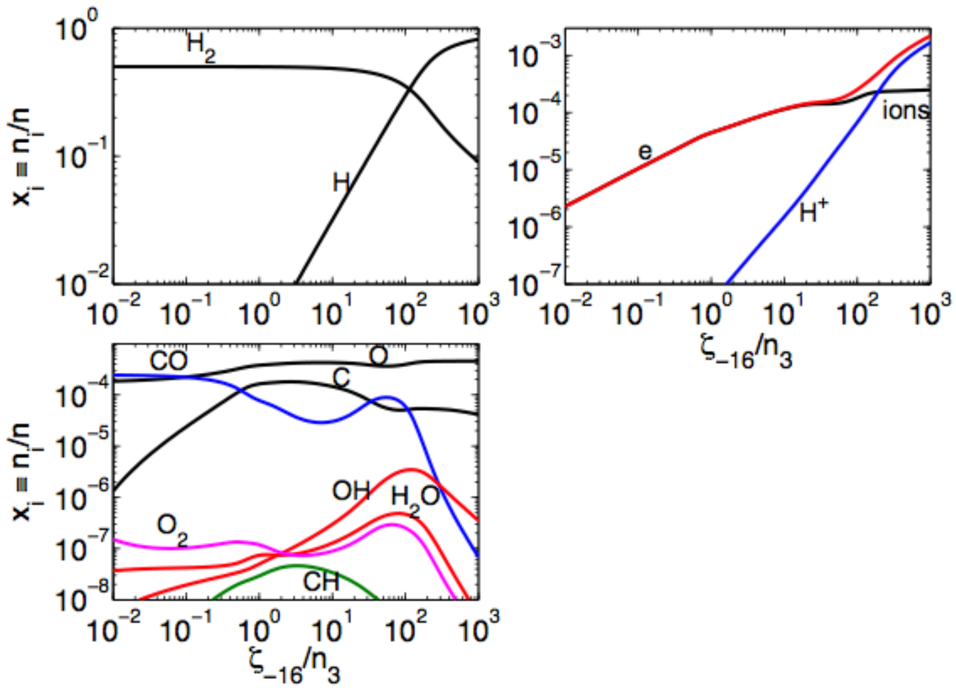

Figure 8. Fractional abundances ($x_i \equiv n_i/n$) as a function of ζ/n for $Z' = 1$, $T_2 = 1$, and $I^0_{\rm UV}/n_3$=0.

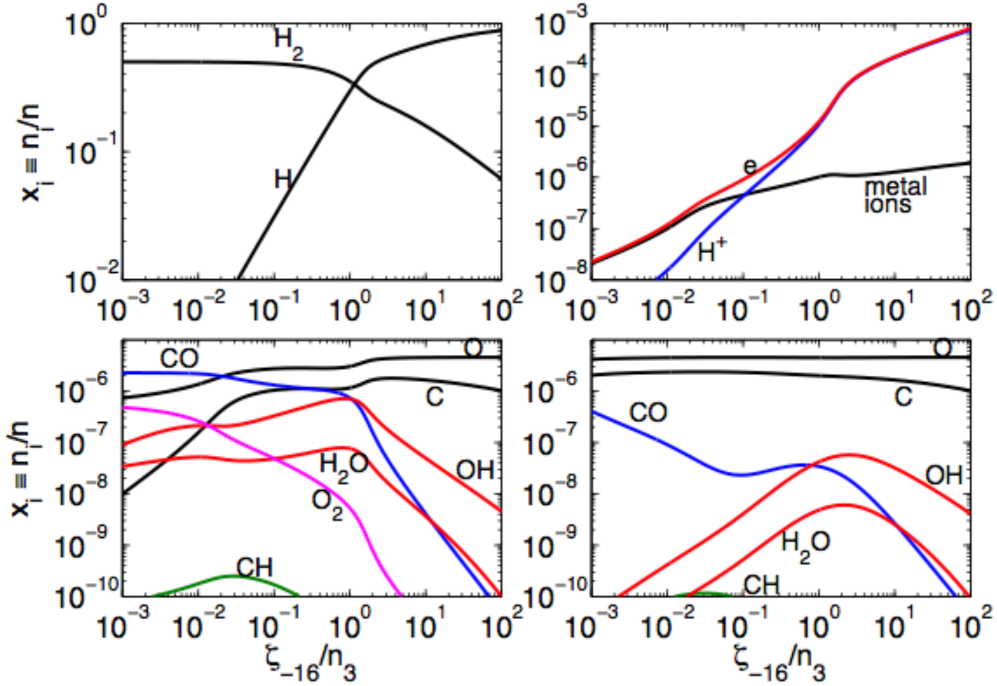

Figure 7. Fractional abundances ($x_i \equiv n_i/n$) as a function of ζ/n for $Z' = 10^{-2}$ and $T_2 = 1$. In the lower right panel $I^0_{\rm UV}/n_3$=1, in all other panels $I^0_{\rm UV}/n_3$=0.

2D - FUV=0

Intro
Model
Results
Summary

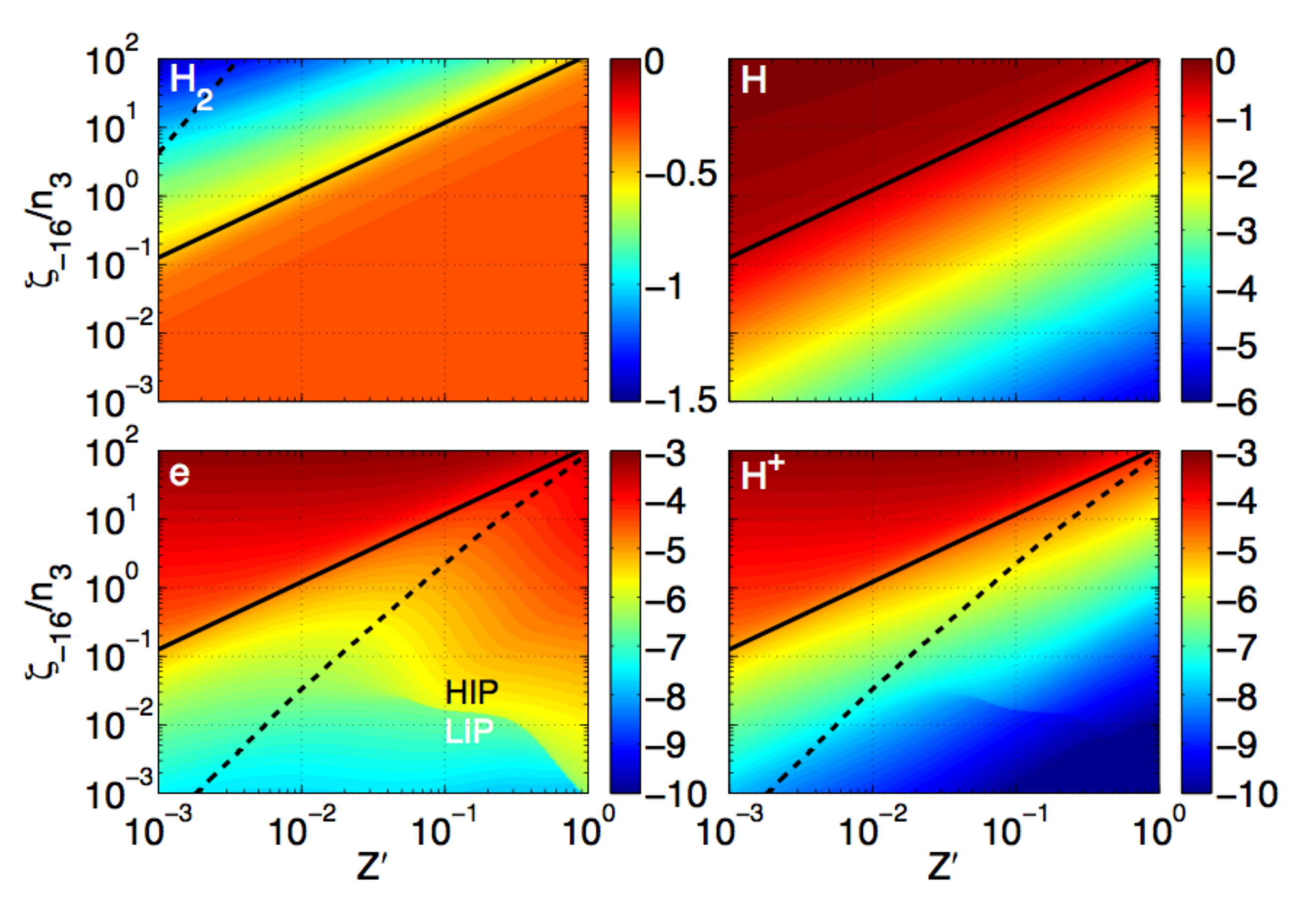

2D - FUV=0

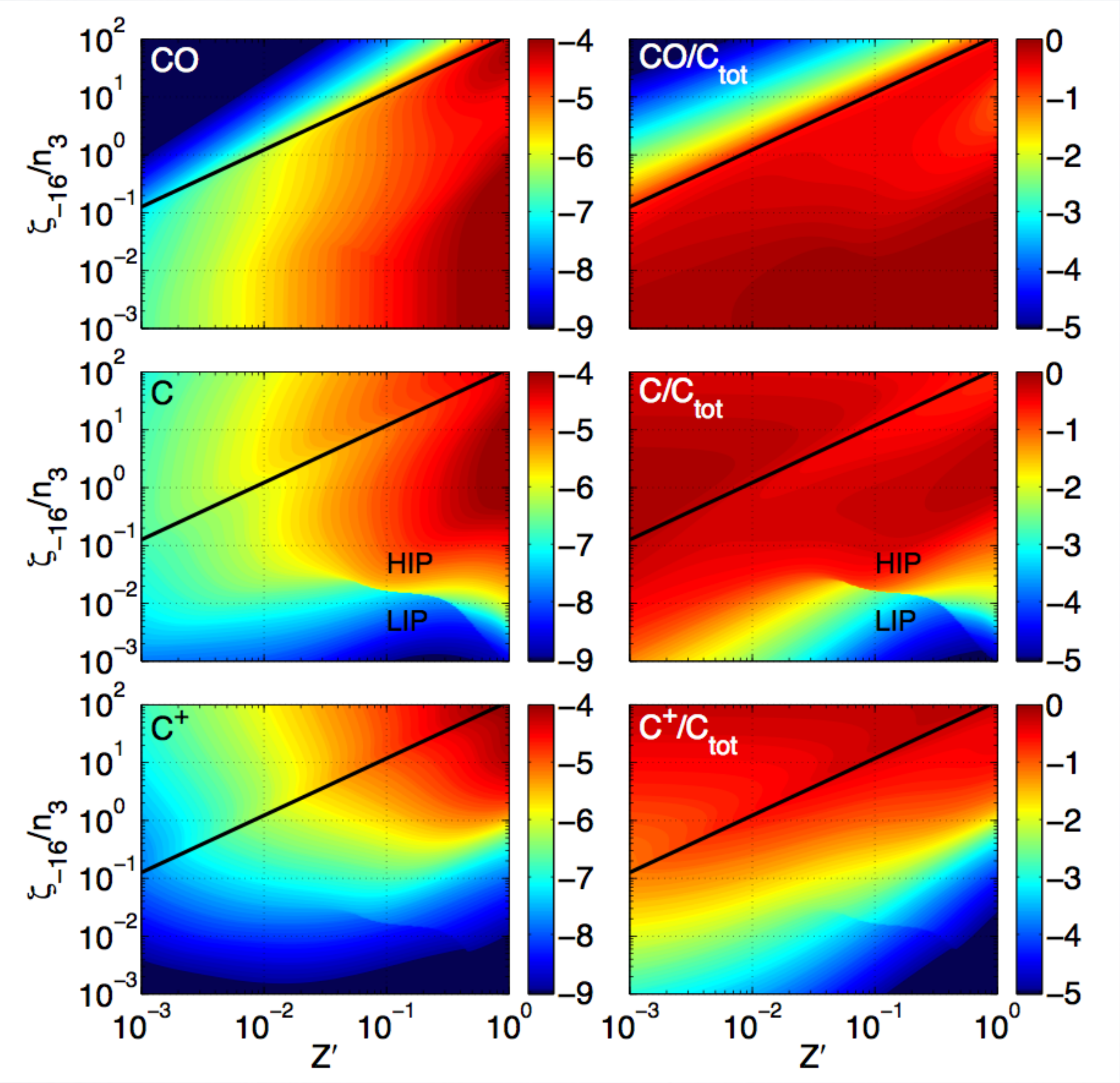

2D - FUV=0

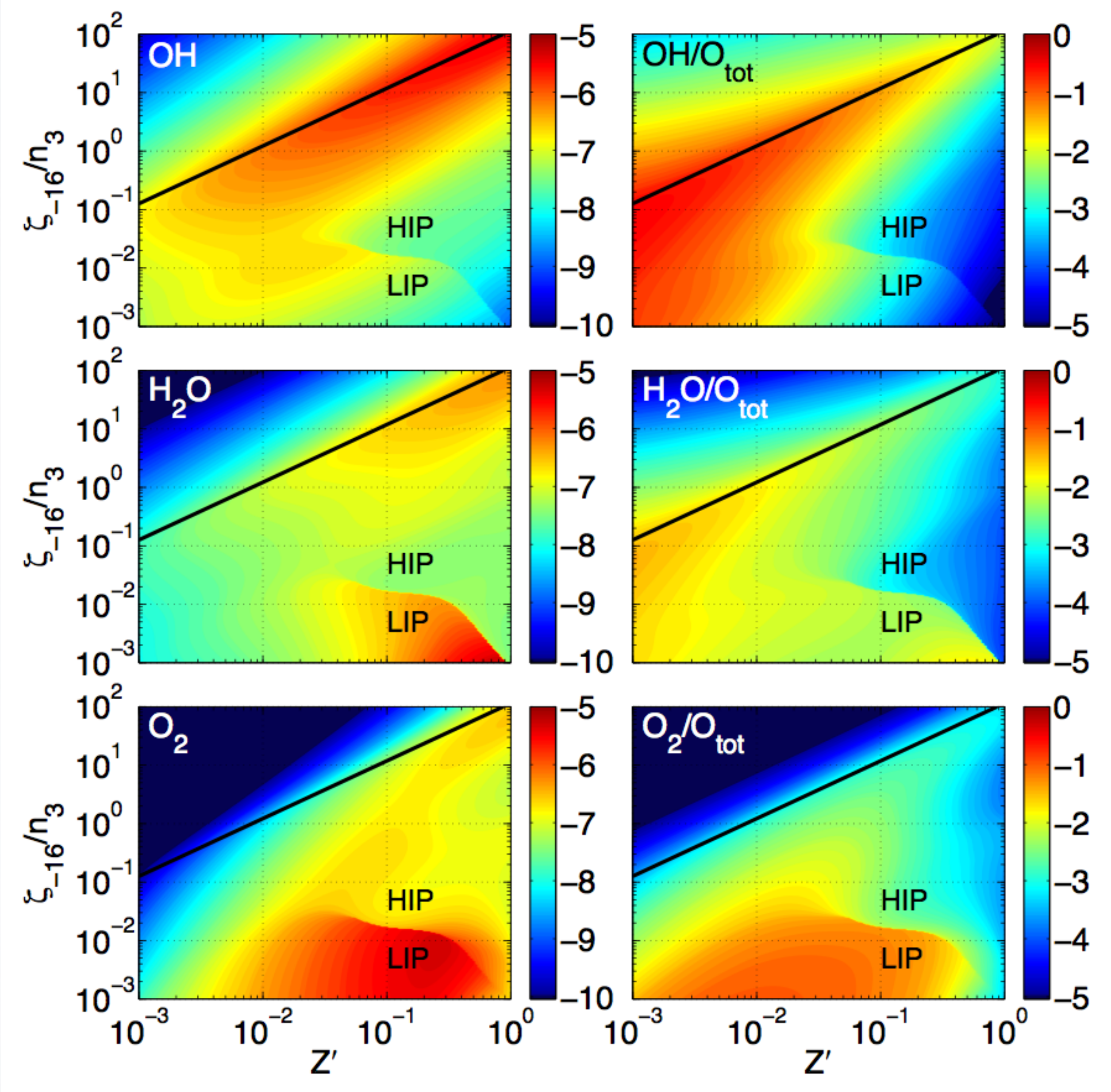
OH
OH/O$_{tot}$
H$_2$O
H$_2$O/O$_{tot}$
O$_2$
O$_2$/O$_{tot}$
HIP
LIP
ζ_{-16}/n_3
Z′
10^{-3}
10^{-2}
10^{-1}
10^{0}
10^{1}
10^{2}
−5
−6
−7
−8
−9
−10
0
−1
−2
−3
−4
−5

2D - FUV=0

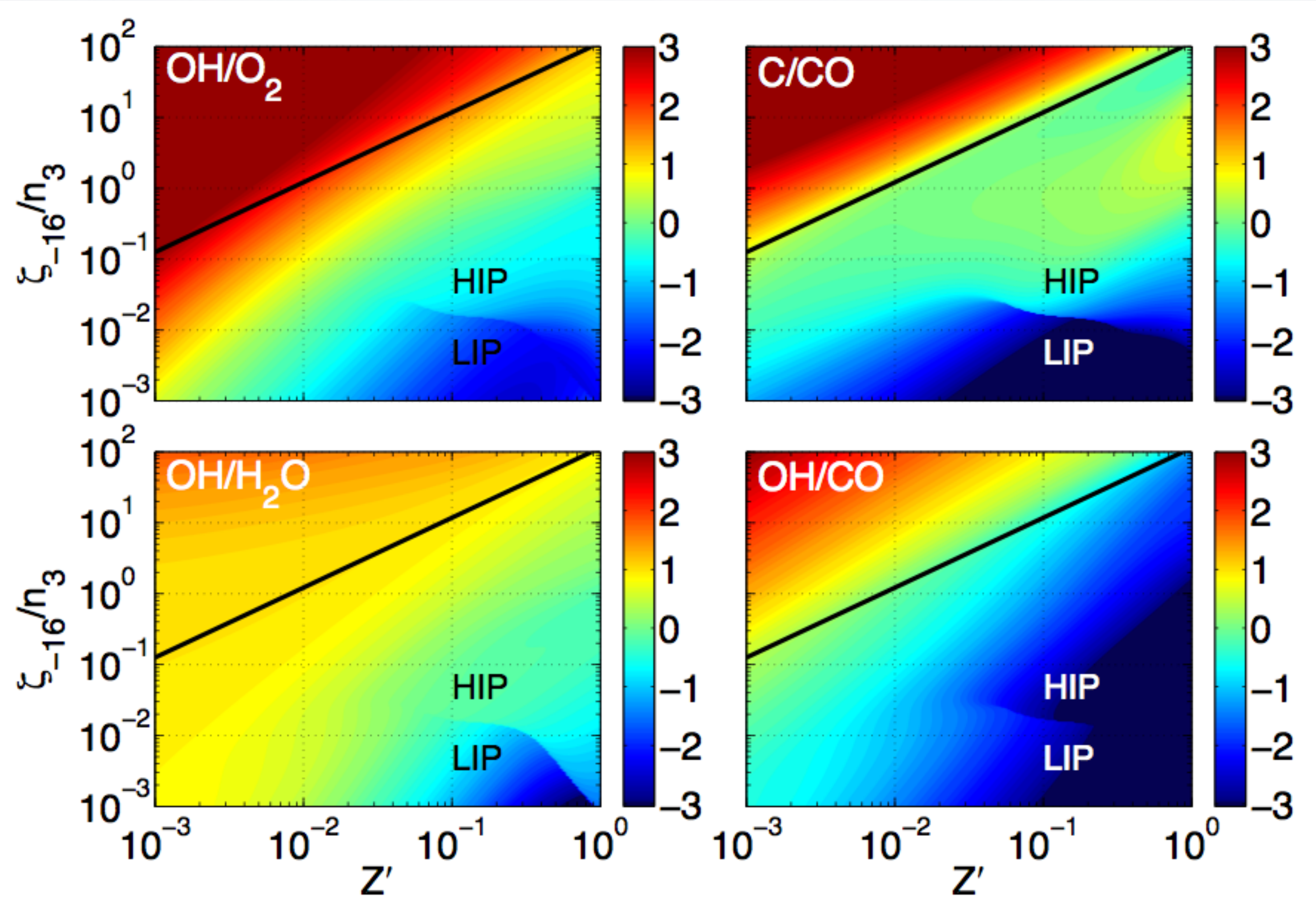

OH/O2
C/CO
OH/H2O
OH/CO
HIP
LIP
HIP
LIP
HIP
LIP
HIP
LIP
ξ−16/n3
ξ−16/n3
Z′
Z′

2D - FUV=0

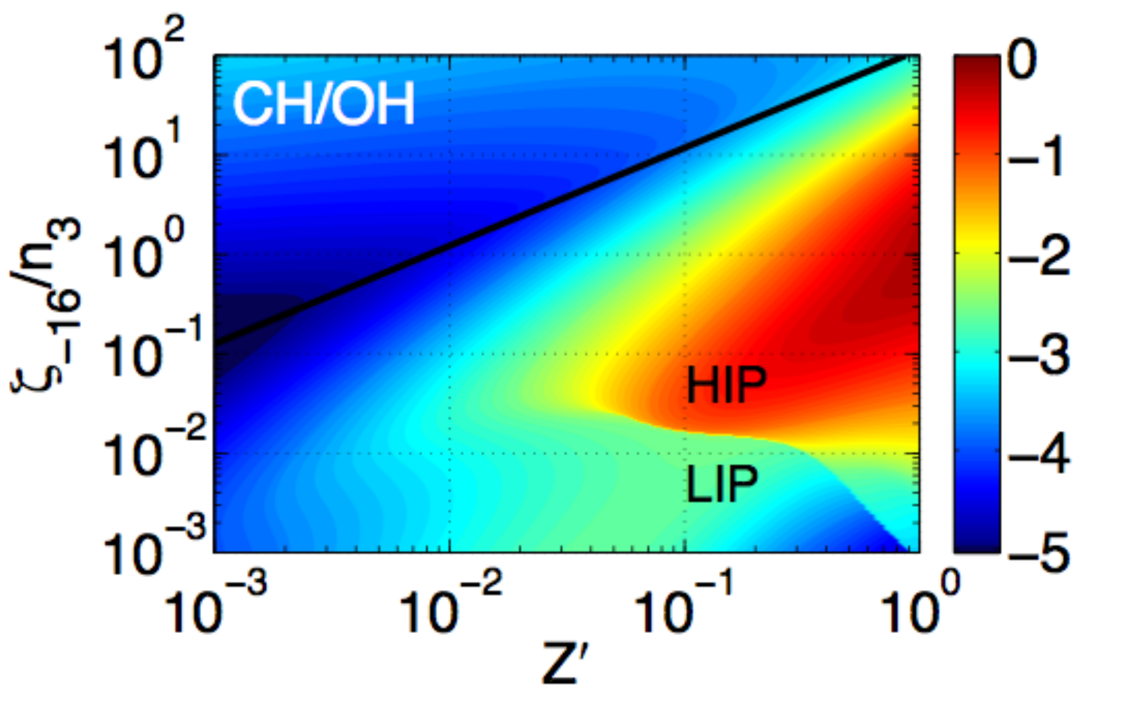

CH/OH
HIP
LIP
ζ_{-16}/n_3
Z′
10^{2}
10^{1}
10^{0}
10^{-1}
10^{-2}
10^{-3}
10^{-3}
10^{-2}
10^{-1}
10^{0}
0
−1
−2
−3
−4
−5

2D - FUV=1

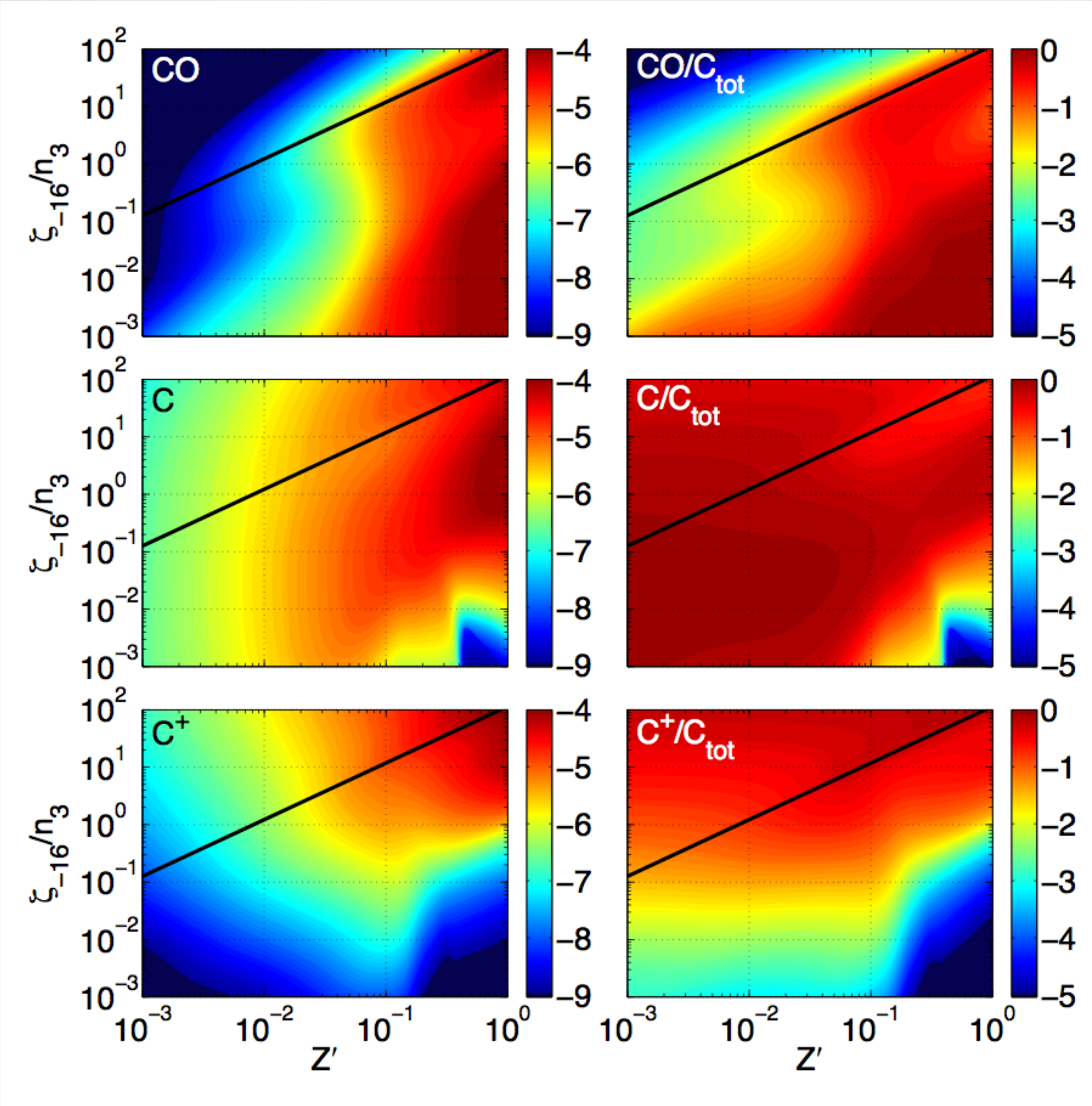
CO
CO/C_tot
C
C/C_tot
C+
C+/C_tot
ζ_−16/n_3
Z′
10^2
10^1
10^0
10^−1
10^−2
10^−3
−4
−5
−6
−7
−8
−9
0
−1
−2
−3
−4
−5

2D - FUV=1

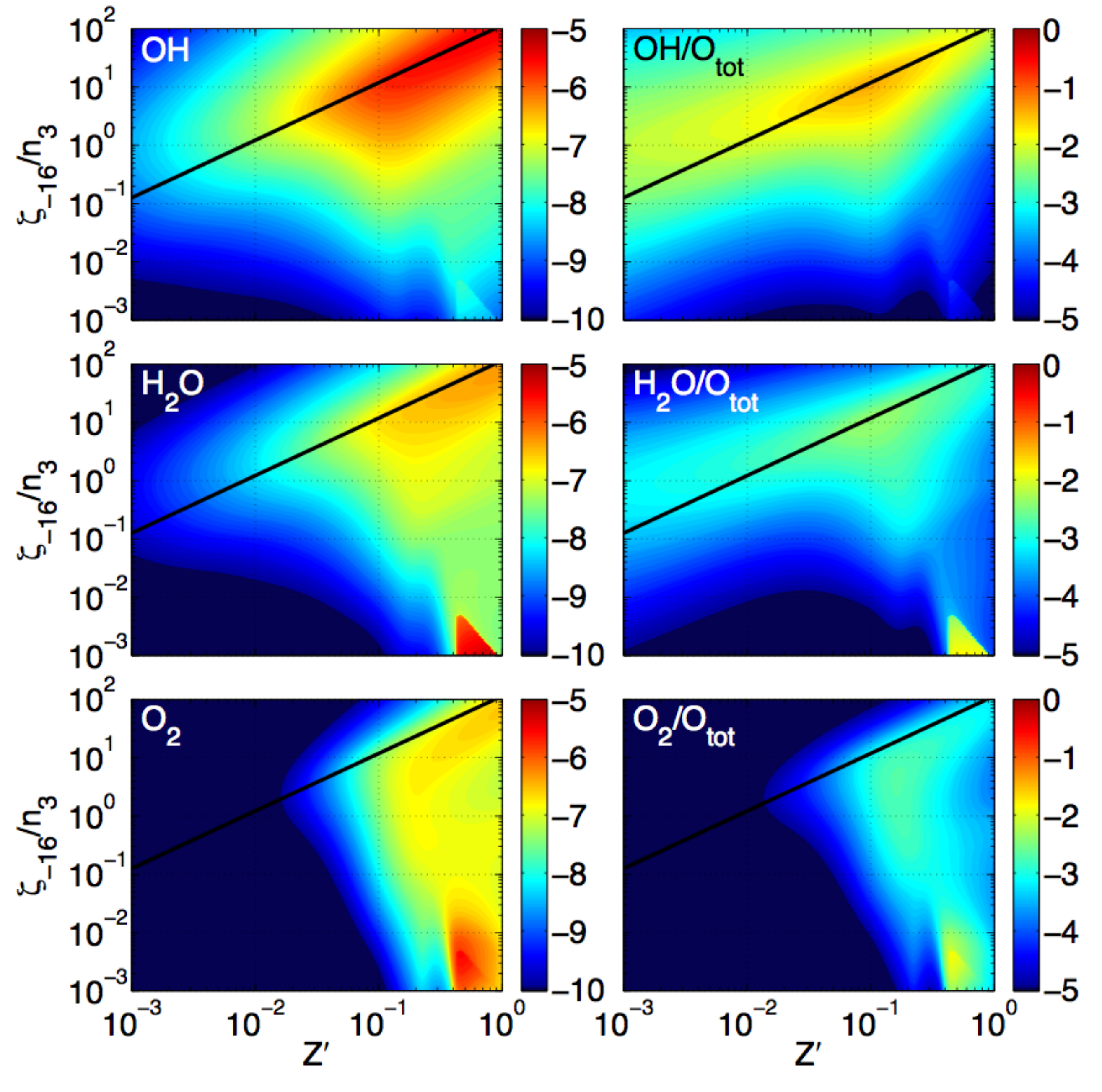

2D - FUV=1